# EDGE-CONTRACTION ON DUAL RIBBON GRAPHS, 2D TQFT, AND THE MIRROR OF ORBIFOLD HURWITZ NUMBERS

OLIVIA DUMITRESCU AND MOTOHICO MULASE

Abstract. We present a new set of axioms for 2D TQFT formulated on the category of cell graphs with edge-contraction operations as morphisms. Given a Frobenius algebra $A$, every cell graph determines an element of the symmetric tensor algebra defined over the dual space $A^*$. We show that the edge-contraction axioms make this assignment equivalent to the TQFT corresponding to $A$. The edge-contraction operations also form an effective tool in various graph enumeration problems, such as counting Grothendieck's dessins d'enfants and simple and double Hurwitz numbers. These counting problems can be solved by the topological recursion, which is the universal mirror B-model corresponding to these counting problems. We show that for the case of orbifold Hurwitz numbers, the mirror objects, i.e., the spectral curves and the differential forms on it, are constructed purely from the edge-contraction operations of the counting problem.

## Contents



## 1. Introduction

The purpose of the present paper is to give a new set of axioms for two-dimensional topological quantum field theory (2D TQFT) formulated in terms of dual ribbon graphs. The key relations between ribbon graphs are **edge-contraction operations**, which correspond to the degenerations in the moduli space $\overline{\mathcal{M}}_{g,n}$ of stable curves of genus $g$ with $n$ labeled points that create a rational component with 3 special points. The structure of Frobenius algebra is naturally encoded in the category of dual ribbon graphs, where edge-contraction operations form morphisms and represent multiplication and comultiplication operations.

2010 *Mathematics Subject Classification.* Primary: 14N35, 81T45, 14N10; Secondary: 53D37, 05A15.

*Key words and phrases.* Topological quantum field theory; topological recursion; Frobenius algebras; ribbon graphs; Hurwitz numbers.

As Grothendieck impressively presents in [16], it is a beautiful and simple yet very surprising idea that a graph drawn on a compact topological surface gives an algebraic structure to the surface. When a positive real number is assigned to each edge as its length, a unique complex structure of the surface is determined. This association leads to a combinatorial model for the moduli space $\mathcal{M}_{g,n}$ of smooth algebraic curves of genus $g$ with $n$ marked points [17, 24, 28, 31, 32]. By identifying these graphs as Feynman diagrams of [34] appearing in the asymptotic expansion of a particular matrix integral, and by giving a graph description of tautological cotangent classes on $\overline{\mathcal{M}}_{g,n}$, Kontsevich [20] shows that Witten's generating function [36] of intersection numbers of these classes satisfies the KdV equations. Kontsevich's argument is based on his discovery that an weighted sum of these intersection numbers is proportional to the Euclidean volume of the combinatorial model of $\mathcal{M}_{g,n}$.

The Euclidean volume of $\mathcal{M}_{g,n}$ depends on the choice of the perimeter length of each face of the graph drawn on a surface. Kontsevich used the *Laplace transform* of the volume as a function of the perimeter length to obtain a set of relations among intersection numbers of different values of $(g, n)$. These relations are equivalent to the conjectured KdV equations.

Recall that if each edge has an integer length, then the resulting Riemann surface by the Strebel correspondence [32] is an algebraic curve defined over $\overline{\mathbb{Q}}$ [3, 24]. Thus a systematic counting of curves defined over $\overline{\mathbb{Q}}$ gives an approximation of the Euclidean volume of Kontsevich by lattice point counting. Since these lattice points naturally correspond to the graphs themselves, the intersection numbers in question can be obtained by graph enumeration, after taking the limit as the mesh length approaches to 0. Now we note that edge-contraction operations give an effective tool for graph enumeration problems. Then one can ask: *what information do the edge-contraction operations tell us about the intersection numbers?*

We found in [11, 12, 25] that the Laplace transform of the counting formula obtained by the edge-contraction operations on graphs is exactly the Virasoro constraint conditions of [7] for the intersection numbers. Indeed it gives the most fundamental example of *topological recursion* of [15].

Euclidean volume is naturally approximated by lattice point counting. It can be also approximated as a limit of hyperbolic volume. The latter idea applied to moduli spaces of hyperbolic surfaces gives the same Virasoro constraint conditions, as beautifully described in the work of Mirzakhani [22, 23]. Mirzakhani's technique of symplectic and hyperbolic geometry can be naturally extended to *character varieties* of surface groups. Yet there are no Virasoro constraints for this type of moduli spaces. We ask: *what do edge-contraction operations give us for the character varieties?*

This is our motivation of the current paper. Instead of discussing the application of our result to character varieties, which will be carried out elsewhere, we focus in this paper our discovery of the relation between edge-contraction operations and 2D TQFT.

Another purpose of this paper is to identify the mirror B-model objects that enable us to solve certain graph enumeration problems. We consider simple and orbifold Hurwitz numbers, by giving a graph enumeration formulation for these numbers. We then show that the mirror of these counting problems are constructed again from the *edge-contraction operations* applied to the genus 0 and one-marked point orbifold Hurwitz numbers. These Hurwitz numbers are the enumeration of certain finite group character varieties for the surface group of a *punctured* Riemann sphere. Of course such an enumeration problem for arbitrary punctured Riemann surfaces forms naturally a 2D TQFT associated with a Frobenius algebra, which is the center of the group algebra of a finite group.

A TQFT of dimension $d$ is a symmetric monoidal functor $Z$ from the monoidal category of $(d-1)$-dimensional compact oriented topological manifolds, with $d$-dimensional oriented cobordism forming morphisms among $(d-1)$-dimensional boundary manifolds, to the monoidal category of finite-dimensional vector spaces defined over a fixed field $K$ [2, 30]. Since there is only one compact manifold in dimension 1, a 2D TQFT is associated with a unique vector space $A = Z(S^1)$, and the Atiyah-Segal axioms of TQFT makes $A$ a commutative Frobenius algebra. It has been established that 2D TQFTs are classified by finite-dimensional Frobenius algebras [1]. We ask the following question, in the reverse direction:

**Question 1.1.** *Suppose we are given a finite-dimensional commutative Frobenius algebra. What is the combinatorial realization of the algebra structure that leads to the corresponding 2D TQFT?*

The answer we propose in this paper is the *category of dual ribbon graphs*, with edge-contraction operations as morphisms. This category does not carry the information of a specific Frobenius algebra. In our forthcoming paper, we will show that our category generates all Frobenius objects among any given monoidal category.

For a given Frobenius algebra $A$ and a ribbon graph $\gamma_{g,n}$ with $n$ vertices drawn on a topological surface of genus $g$, we assign a multilinear map

$$\gamma_{g,n} : A^{\otimes n} \longrightarrow K.$$

The *edge-contraction axioms* of Section 4 determine the behavior of this map under the change of ribbon graphs via edge contractions. Theorem 4.7, our main result of this paper, exhibits a surprising statement that the map $\gamma_{g,n}$ depends only on $g$ and $n$, and is independent of the choice of the graph $\gamma_{g,n}$. We then evaluate $\gamma_{g,n}$ for each $v_1 \otimes \cdots \otimes v_n \in A^{\otimes n}$ and prove that this map indeed defines the TQFT corresponding to $A$.

A *ribbon graph* (also called as a dessin d'enfant, fatgraph, embedded graph, or a map) is a graph with an assignment of a cyclic order of half-edges incident at each vertex. The cyclic order induces the ribbon structure to the graph, and it becomes the 1-skeleton of the cell-decomposition of a compact oriented topological surface of genus, say $g$, by attaching oriented open discs to the graph. Let $n$ be the number of the discs attached. We call this ribbon graph of *type* $(g, n)$.

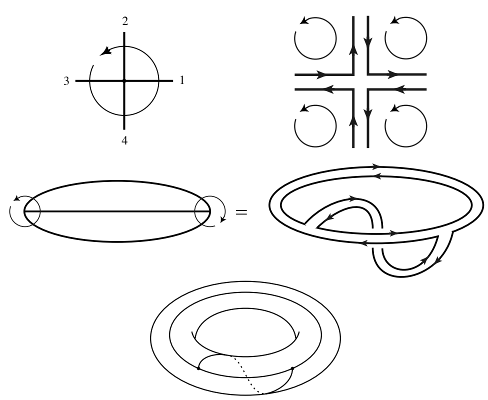


FIGURE 1.1. Top Row: A cyclic order of half-edges at a vertex induces a local ribbon structure to a graph. Second Row: Globally, a ribbon graph is the 1-skeleton of a cell-decomposition of a compact oriented surface. Third Row: A ribbon graph is thus a graph drawn on a compact oriented surface.

An assignment of a positive real number to each edge of a ribbon graph determines a concrete holomorphic coordinate system of the topological surface of genus $g$ with $n$

labeled marked points [24], thus making it a Riemann surface. This construction gives the identification of the space of ribbon graphs of type $(g,n)$ with positive edge lengths assigned, and the space $\mathcal{M}_{g,n}\times\mathbb{R}_+^n$, as an orbifold. The operation of edge-contraction of an edge connecting two distinct vertices then defines the boundary operator, which introduces the structure of orbi-cell complex on $\mathcal{M}_{g,n}\times\mathbb{R}_+^n$. Each ribbon graph determines the stratum of this cell complex, whose dimension is the number of edges of the graph.

Since the ribbon graphs we need for the consideration of TQFT have *labeled vertices* but no labels for faces, we use the terminology **cell graph of type** $(g,n)$ for a ribbon graph of genus $g$ with $n$ labeled vertices. A cell graph of type $(g,n)$ is the dual of a ribbon graph of the same type $(g,n)$. The set of all cell graphs of type $(g,n)$ is denoted by $\Gamma_{g,n}$.

Ribbon graphs naturally form orbi-cell complex. Their dual cell graphs naturally form a category $\mathcal{CG}$, as we shall define in Section 5. We then consider functors

$$\omega : \mathcal{CG} \longrightarrow \mathcal{F}un(\mathcal{C}/K,\mathcal{C}/K),$$

where $(\mathcal{C},\otimes,K)$ is a monoidal category with the unit object $K$, and $\mathcal{F}un(\mathcal{C}/K,\mathcal{C}/K)$ is the endofunctor category over the category of $K$-objects of $\mathcal{C}$. Each cell graph corresponds to an endofunctor, and edge-contraction operations among them correspond to natural transformations. Our consideration can be generalized to the cohomological field theory of Kontsevich-Manin [21]. After this generalization, we can construct a functor that gives a classification of 2D TQFT. Since we need more preparation, these topics will be discussed in our forthcoming paper.

Edge-contraction operations also provide an effective method for graph enumeration problems. It has been noted in [12] that the Laplace transform of edge-contraction operations on many counting problems corresponds to the topological recursion of [15]. In the second part of this paper, we examine the construction of the mirror B-models corresponding to the simple and orbifold Hurwitz numbers.

In general, enumerative geometry problems, such as computation of Gromov-Witten type invariants, are solved by studying a corresponding problem on the *mirror dual* side. The effectiveness of the mirror problem relies on the technique of complex analysis. The second question we consider in this paper is the following:

**Question 1.2.** *How do we find the mirror of a given enumerative problem?*

We give an answer to this question for a class of graph enumeration problems that are equivalent to counting of orbifold Hurwitz numbers. The key is again the same edge-contraction operations. The base case, or the case for the "moduli space" $\overline{\mathcal{M}}_{0,1}$, of the edge contraction in the counting problem identifies the mirror dual object, and a universal mechanism of complex analysis, known as the **topological recursion** of [15], solves the B-model side of the counting problem. The solution is a collection of generating functions of the original problem for all genera.

To illustrate the idea, let us consider the number $T_d$ of connected *trees* consisting of *labeled* $d$ nodes (or vertices). The initial condition is $T_1 = 1$. The numbers satisfy a recursion relation

$$(d-1)T_d = \frac{1}{2}\sum_{\substack{a+b=d\\ a,b\geq 1}} ab\binom{d}{a}T_aT_b. \tag{1.1}$$

A tree of $d$ nodes has $d-1$ edges. The left-hand side counts how many ways we can eliminate an edge. When an edge is eliminated, the tree breaks down into two disjoint pieces, one consisting of $a$ labeled nodes, and the other $b = d-a$ labeled nodes. The original tree is restored by connecting one of the $a$ nodes on one side to one of the $b$ nodes on the other side. The equivalence of counting in this elimination process gives (1.1). From the initial value, the recursion formula generates the tree sequence $1, 1, 3, 16, 125, 1296, \dots$. We note, however, that (1.1) does not directly give a closed formula for $T_d$. To find one, we introduce a generating function, or a **spectral curve**

$$y = y(x) := \sum_{d=1}^{\infty} \frac{T_d}{(d-1)!} x^d. \tag{1.2}$$

Then (1.1) is equivalent to

$$\left( x^2 \circ \frac{d}{dx} \circ \frac{1}{x} \right) y = \frac{1}{2} x \frac{d}{dx} y^2. \tag{1.3}$$

The initial condition is $y(0) = 0$ and $y'(0) = 1$, which solves the differential equation uniquely as

$$x = ye^{-y}. \tag{1.4}$$

This is a plane analytic curve known as the *Lambert curve.* To find the formula for $T_d$, we need the *Lagrange Inversion Formula.* Suppose that $f(y)$ is a holomorphic function defined near $y = 0$, and that $f(0) \neq 0$. Then the inverse function of $x = \frac{y}{f(y)}$ near $x = 0$ is given by

$$y = \sum_{k=1}^{\infty} \left( \frac{d}{dy} \right)^{k-1} \left( f(y)^k \right) \Bigg|_{y=0} \frac{x^k}{k!}. \tag{1.5}$$

The proof is elementary and requires only Cauchy's integration formula. Since $f(y) = e^y$ in our case, we immediately obtain Cayley's formula $T_d = d^{d-2}$.

The point we wish to make here is that the real problem behind the scene is not tree-counting, but *simple Hurwitz numbers.* This relation is understood by the correspondence between trees and ramified coverings of $\mathbb{P}^1$ by $\mathbb{P}^1$ of degree $d$ that are simply ramified except for one total ramification point. When we look at the dual graph of a tree, the edge elimination becomes the edge-contraction operation, and this operation precisely gives a *degeneration formula* for counting problems on $\overline{\mathcal{M}}_{g,n}$. The base case for the counting problem is $(g, n) = (0, 1)$, and the recursion (1.1) is the result of the edge-contraction operation for simple Hurwitz numbers associated with $\overline{\mathcal{M}}_{0,1}$. Here, the Lambert curve (1.4) is the *mirror dual* of simple Hurwitz numbers.

In the dual picture, $T_d$ counts the number of cell-decompositions of a sphere $S^2$ consisting of one 0-cell, $(d-1)$ 1-cells, and $d$ labeled 2-cells. The edge-contraction operation causes the degeneration of $\mathbb{P}^1$ with one marked point $p$ into two $\mathbb{P}^1$'s with one marked point on each, connected by a $\mathbb{P}^1$ with 3 special points, two of which are nodal points and the third one representing the original marked point $p$. In terms of graph enumeration, the $\mathbb{P}^1$ with 3 special points does not play any role. So we break the original vertex into two vertices, and separate the graph into two disjoint pieces (Figure 1.2).

Bouchard and Mariño [5] conjectured that generating functions for simple Hurwitz numbers could be calculated by the topological recursion of [15], based on the spectral curve (1.4). Here, the notion of spectral curve is the mirror dual object for the counting problem. They arrived at the mirror dual by a consideration of mirror symmetry of toric Calabi-Yau three-folds. The conjecture was solved in a series of papers of one of the authors [14, 27], using the Lambert curve as the mirror. The emphasis of our current paper is that the mirror dual object is simply a consequence of the $\overline{\mathcal{M}}_{0,1}$ case of the edge-contraction operation

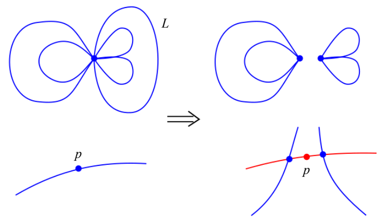


FIGURE 1.2. The edge-contraction operation on a loop is a degeneration process. The graph on the left is a connected cell graph of type $(0,1)$. The edge-contraction on the loop $L$ changes it to the one on the right. Here, a $\mathbb{P}^1$ with one marked point $p$ degenerates into two $\mathbb{P}^1$'s with one marked point on each, connected by a $\mathbb{P}^1$ with 3 special points.

on the original counting problem. The situation is similar to several cases of Gromov-Witten theory, where the mirror is constructed by the genus 0 Gromov-Witten invariants themselves.

Once we have our formulation of 2D TQFT and topological recursion in terms of edge-contraction operations, we can consider a TQFT-valued topological recursion. An immediate example is the Gromov-Witten theory of the classifying space $BG$ of a finite group $G$. In our forthcoming paper, we will show that a straightforward generalization of the topological recursion for differential forms with values in tensor products of a Frobenius algebra automatically splits into the product of the usual scalar-valued solution to the topological recursion and a 2D TQFT. Therefore, topological recursion implies TQFT. Here, we remark the similarity between the topological recursion and the comultiplication operation in a Frobenius algebra. Indeed, the topological recursion itself can be regarded as a comultiplication formula for an infinite-dimensional analogue of the Frobenius algebra (Vertex algebras, or conformal field theory).

The authors have noticed that the topological recursion appears as the Laplace transform of edge-contraction operations in [12]. The geometric nature of the topological recursion was further investigated in [9, 10], where it was placed in the context of Hitchin spectral curves for the first time, and the relation to quantum curves was discovered. The present paper is the authors' first step toward identifying the topological recursion in an algebraic and categorical setting. We note that Hitchin moduli spaces are diffeomorphic to character varieties of a surface group. The TQFT point of view of our current paper in the context of these character varieties, in particular, their Hodge structures, will be discussed elsewhere.

The paper is organized as follows. We start with a quick review of Frobenius algebras, for the purpose of setting notations, in Section 2. We then recall two-dimensional TQFT in Section 3. In Sections 4, we give our formulation of 2D TQFT in terms of the edge-contraction axioms of cell graphs. A categorical formulation of our axioms is given in Section 5. In Section 6, we present combinatorial graph enumeration problems, and show that they are equivalent to counting of simple and orbifold Hurwitz numbers. Finally in Section 7, the spectral curves of the topological recursion for simple and orbifold Hurwitz numbers (the mirror objects to the counting problems) are constructed from the edge-contraction formulas for $(g,n) = (0,1)$ invariants.

## 2. Frobenius algebras

In this paper, we are concerned with finite-dimensional, unital, commutative Frobenius algebras defined over a field $K$. In this section we review the necessary account of Frobenius algebra and set notations.

Let $A$ be a finite-dimensional, unital, associative, and commutative algebra over a field $K$. A non-degenerate bilinear form $\eta : A \otimes A \longrightarrow K$ is a *Frobenius form* if

$$\eta\big(v_1, m(v_2, v_3)\big) = \eta\big(m(v_1, v_2), v_3\big), \qquad v_1, v_2, v_3 \in A, \tag{2.1}$$

where $m : A \otimes A \longrightarrow A$ is the multiplication. We denote by

$$\lambda : A \overset{\sim}{\longrightarrow} A^*, \qquad \langle \lambda(u), v\rangle = \eta(u, v), \tag{2.2}$$

the canonical isomorphism of the algebra A and its dual. We assume that $\eta$ is a symmetric bilinear form. Let $\mathbf{1} \in A$ denote the multiplicative identity. Then it defines a *counit*, or a *trace*, by

$$\epsilon : A \longrightarrow K, \qquad \epsilon(v) = \eta(\mathbf{1}, v). \tag{2.3}$$

The canonical isomorphism $\lambda$ introduces a unique cocommutative and coassociative coalgebra structure in $A$ by the following commutative diagram.

$$\begin{array}{ccc} A & \xrightarrow{\ \delta\ } & A \otimes A \\ {\scriptstyle\lambda}\big\downarrow & & \big\downarrow{\scriptstyle\lambda\otimes\lambda} \\ A^* & \xrightarrow[\ m^*\ ]{} & A^* \otimes A^* \end{array} \tag{2.4}$$

It is often convenient to use a basis for calculations. Let $\langle e_1, e_2, \dots, e_r\rangle$ be a $K$-basis for $A$. In terms of this basis, the bilinear form $\eta$ is identified with a symmetric matrix, and its inverse is written as follows:

$$\eta = [\eta_{ij}], \qquad \eta_{ij} := \eta(e_i, e_j), \qquad \eta^{-1} = [\eta^{ij}]. \tag{2.5}$$

The comultiplication is then written as

$$\delta(v) = \sum_{i,j,a,b} \eta\big(v, m(e_i, e_j)\big)\eta^{ia}\eta^{jb} e_a \otimes e_b.$$

From now on, if there is no confusion, we denote simply by $m(u, v) = uv$. The symmetric Frobenius form and the commutativity of the multiplication makes

$$\eta\big(e_{i_1} \cdots e_{i_j}, e_{i_{j+1}} \cdots e_n\big) = \epsilon(e_{i_1} \cdots e_{i_n}), \qquad 1 \le j < n, \tag{2.6}$$

completely symmetric with respect to permutations of the indices.

The following is a standard formula for a non-degenerate bilinear form:

$$v = \sum_{a,b} \eta(v, e_a)\eta^{ab} e_b. \tag{2.7}$$

It immediately follows that

**Lemma 2.1.** *The following diagram commutes:*

$$
\begin{tikzcd}
 & A\otimes A\otimes A \arrow[dr, "m\otimes id"] & \\
A\otimes A \arrow[ur, "id\otimes\delta"] \arrow[r, "m"] \arrow[dr, "\delta\otimes id"'] & A \arrow[r, "\delta"] & A\otimes A. \\
 & A\otimes A\otimes A \arrow[ur, "id\otimes m"'] &
\end{tikzcd}
\tag{2.8}
$$

*Or equivalently, for every $v_1, v_2$ in $A$, we have*

$$\delta(v_1v_2) = (id\otimes m)\big(\delta(v_1), v_2\big) = (m\otimes id)\big(v_2, \delta(v_1)\big).$$

*Proof.* Noticing the commutativity and cocommutativity of $A$, we have

$$
\begin{aligned}
\delta(v_1v_2) &= \sum_{i,j,a,b} \eta(v_1v_2, e_ie_j)\eta^{ia}\eta^{jb}e_a\otimes e_b \\
&= \sum_{i,j,a,b} \eta(v_1e_i, v_2e_j)\eta^{ia}\eta^{jb}e_a\otimes e_b \\
&= \sum_{i,j,a,b,c,d} \eta(v_1e_i, e_c)\eta^{cd}\eta(e_d, v_2e_j)\eta^{ia}\eta^{jb}e_a\otimes e_b \\
&= \sum_{i,j,a,b,c,d} \eta(v_1, e_ie_c)\eta^{cd}\eta^{ia}\eta(e_dv_2, e_j)\eta^{jb}e_a\otimes e_b \\
&= \sum_{i,a,c,d} \eta(v_1, e_ie_c)\eta^{cd}\eta^{ia}e_a\otimes (e_dv_2) \\
&= (id\otimes m)\big(\delta(v_1), v_2\big).
\end{aligned}
$$

□

In the lemma above we consider the composition $\delta\circ m$. The other order of operations plays an essential role in 2D TQFT.

**Definition 2.2** (Euler element)**.** The **Euler element** of a Frobenius algebra $A$ is defined by

$$\mathbf{e} := m\circ\delta(\mathbf{1}). \tag{2.9}$$

In terms of basis, the Euler element is given by

$$\mathbf{e} = \sum_{a,b} \eta^{ab}e_ae_b. \tag{2.10}$$

Another application of (2.7) is the following formula that relates the multiplication and comultiplication.

$$(\lambda(v_1)\otimes id)\,\delta(v_2) = v_1v_2. \tag{2.11}$$

This is because

$$
\begin{aligned}
(\lambda(v_1)\otimes id)\,\delta(v_2) &= \sum_{a,b,k,\ell} (\lambda(v_1)\otimes id)\,\eta(v_2, e_ke_\ell)\eta^{ka}\eta^{\ell b}e_a\otimes e_b \\
&= \sum_{a,b,k,\ell} \eta(v_2e_\ell, e_k)\eta^{ka}\eta(v_1, e_a)\eta^{\ell b}e_b
\end{aligned}
$$

$$= \sum_{b,\ell} \eta(v_1, v_2 e_\ell)\eta^{\ell b} e_b = v_1 v_2.$$

## 3. 2D TQFT

The axiomatic formulation of conformal and topological quantum field theories was established in 1980s. We refer to Atiyah [2] and Segal [30]. We consider only two-dimensional topological quantum field theories in this paper. Again for the purpose of setting notations, we provide a brief review of the subject in this section, even though it is discussed in many literature, including [19].

A 2D TQFT is a symmetric monoidal functor $Z$ from the cobordism category of oriented surfaces (a surface being a cobordism of its boundary circles) to the monoidal category of finite-dimensional vector spaces over a fixed field $K$ with the operation of tensor products. The Atiyah-Segal TQFT axioms automatically make the vector space

$$Z(S^1) = A \tag{3.1}$$

a unital commutative Frobenius algebra over $K$.

Let $\Sigma_{g,n}$ be an oriented surface of finite topological type $(g, n)$, i.e., a surface obtained by removing $n$ disjoint open discs from a compact oriented two-dimensional topological manifold of genus $g$. The boundary components are labeled by indices $1, \dots, n$. We always give the induced orientation at each boundary circle. The TQFT then assigns to such a surface a multilinear map

$$\Omega_{g,n} \overset{\text{def}}{=} Z(\Sigma_{g,n}) : A^{\otimes n} \longrightarrow K. \tag{3.2}$$

If we change the orientation at the $i$-th boundary, then the $i$-th factor of the tensor product is changed to the dual space $A^*$. Therefore, if we have $k$ boundary circles with induced orientation and $\ell$ circles with opposite orientation, then we have a multi-linear map

$$\Omega_{g,k,\bar{\ell}} : A^{\otimes k} \longrightarrow A^{\otimes \ell}.$$

The sewing axiom of Atiyah [2] requires that

$$\Omega_{g_2,\ell,\bar{n}} \circ \Omega_{g_1,k,\bar{\ell}} = \Omega_{g_1+g_2+\ell-1,k,\bar{n}} : A^{\otimes k} \longrightarrow A^{\otimes n}.$$

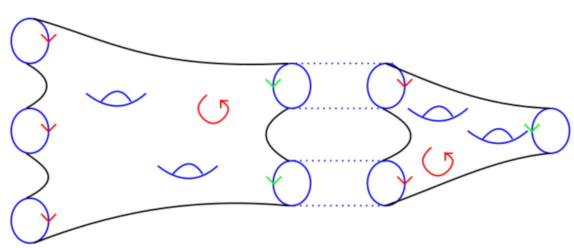

FIGURE 3.1.

A 2D TQFT can be also obtained as a special case of a CohFT of [21].

**Definition 3.1** (Cohomological Field Theory)**.** We denote by $\overline{\mathcal{M}}_{g,n}$ the moduli space of stable curves of genus $g \geq 0$ and $n \geq 1$ smooth marked points subject to the stability condition $2g - 2 + n > 0$. Let

$$\pi : \overline{\mathcal{M}}_{g,n+1} \longrightarrow \overline{\mathcal{M}}_{g,n} \tag{3.3}$$

be the forgetful morphism of the last marked point, and

$$gl_1 : \overline{\mathcal{M}}_{g-1,n+2} \longrightarrow \overline{\mathcal{M}}_{g,n} \tag{3.4}$$

$$gl_2 : \overline{\mathcal{M}}_{g_1,n_1+1} \times \overline{\mathcal{M}}_{g_2,n_2+1} \longrightarrow \overline{\mathcal{M}}_{g_1+g_2,n_1+n_2} \tag{3.5}$$

the gluing morphisms that give boundary strata of the moduli space. An assignment

$$\Omega_{g,n} : A^{\otimes n} \longrightarrow H^*(\overline{\mathcal{M}}_{g,n}, K) \tag{3.6}$$

is a CohFT if the following axioms hold:

**CohFT 0:** $\Omega_{g,n}$ is $S_n$-invariant, i.e., symmetric, and $\Omega_{0,3}(\mathbf{1}, v_1, v_2) = \eta(v_1, v_2)$.

**CohFT 1:** $\Omega_{g,n+1}(v_1, \ldots, v_n, \mathbf{1}) = \pi^*\Omega_{g,n}(v_1, \ldots, v_n)$.

**CohFT 2:** $gl_1^*\Omega_{g,n}(v_1, \ldots, v_n) = \sum_{a,b} \Omega_{g-1,n+2}(v_1, \ldots, v_n, e_a, e_b)\eta^{ab}$.

**CohFT 3:** $gl_2^*\Omega_{g_1+g_2,|I|+|J|}(v_I, v_J) = \sum_{a,b} \Omega_{g_1,|I|+1}(v_I, e_a)\Omega_{g_2,|J|+1}(v_J, e_b)\eta^{ab}$,

where $I \sqcup J = \{1, \ldots, n\}$.

If a CohFT takes values in $H^0(\overline{\mathcal{M}}_{g,n}, K) = K$, then it is a 2D TQFT. In what follows, we only consider CohFT with values in $H^0(\overline{\mathcal{M}}_{g,n}, K)$.

**Remark 3.2.** The forgetful morphism makes sense for a stable pointed curve, but it does not exist for a topological surface with boundary in the same way. Certainly we cannot just *forget* a boundary. For a TQFT, eliminating a boundary corresponds to capping a disc. In algebraic geometry language, it is the same as gluing a component of $g = 0$ and $n = 1$. Since $H^0(\overline{\mathcal{M}}_{g,n}, K) = K$ is not affected by the morphism (3.3)-(3.5), the equation

$$\Omega_{g,n}(\mathbf{1}, v_2, \ldots, v_n) = \Omega_{g,n-1}(v_2, \ldots, v_n)$$

is identified with CohFT 3 for $g_2 = 0$ and $J = \emptyset$, if we define

$$\Omega_{0,1}(v) := \epsilon(v) = \eta(\mathbf{1}, v), \tag{3.7}$$

even though $\overline{\mathcal{M}}_{0,1}$ does not exist. We then have

$$\begin{aligned}\Omega_{g,n}(v_1, \ldots, v_n) &= \sum_{a,b} \Omega_{g,n+1}(v_1, \ldots, v_n, e_a)\eta(\mathbf{1}, e_b)\eta^{ab} \\ &= \Omega_{g,n+1}(v_1, \ldots, v_n, \mathbf{1})\end{aligned}$$

by (2.7). In other words, the isomorphism of the degree 0 cohomologies

$$\pi^* : H^0(\overline{\mathcal{M}}_{g,n}, K) \longrightarrow H^0(\overline{\mathcal{M}}_{g,n+1}, K) \tag{3.8}$$

is replaced by its left inverse

$$\sigma_i^* : H^0(\overline{\mathcal{M}}_{g,n+1}, K) \longrightarrow H^0(\overline{\mathcal{M}}_{g,n}, K), \tag{3.9}$$

where

$$\sigma_i : \overline{\mathcal{M}}_{g,n} \longrightarrow \overline{\mathcal{M}}_{g,n+1} \tag{3.10}$$

is one of the $n$ tautological sections. Of course this consideration does not apply for CohFT.

**Remark 3.3.** In the same spirit, although $\overline{\mathcal{M}}_{0,2}$ does not exist either, we can *define*

$$\Omega_{0,2}(v_1, v_2) := \eta(v_1, v_2) \tag{3.11}$$

so that we exhaust all cases appearing in the Atiyah-Segal axioms for 2D TQFT. In particular, for $g_2 = 0$ and $J = \{n\}$, we have

$$\begin{aligned}\Omega_{g,n}(v_1, \dots, v_n) &= \Omega_{g,n}\left(v_1, \dots, v_{n-1}, \sum_{a,b} \eta(v_n, e_b)\eta^{ab} e_a\right) \\ &= \sum_{a,b} \Omega_{g,n}(v_1, \dots, v_{n-1}, e_a)\Omega_{0,2}(v_n, e_b)\eta^{ab}.\end{aligned}$$

Thus $\Omega_{0,2}(v_1, v_2)$ functions as the identity operator of the Atiyah-Segal axiom [2].

**Remark 3.4.** A marked point $p_i$ of a stable curve $\Sigma \in \overline{\mathcal{M}}_{g,n}$ is an insertion point for the cotangent class $\psi_i = c_1(\mathbb{L}_i)$, where $\mathbb{L}_i$ is the pull-back of the relative canonical sheaf on the universal curve $\pi : \overline{\mathcal{M}}_{g,n+1} \longrightarrow \overline{\mathcal{M}}_{g,n}$ by the $i$-th tautological section $\sigma_i : \overline{\mathcal{M}}_{g,n} \longrightarrow \overline{\mathcal{M}}_{g,n+1}$. If we cut a small disc around $p_i \in \Sigma$, then the orientation induced on the boundary circle is consistent with the orientation of the unit circle in $T^*_{p_i}\Sigma$. This orientation is opposite to the orientation that is naturally induced on $T_{p_i}\Sigma$. In general, if $V$ is an oriented real vector space of dimension $n$, then $V^*$ naturally acquires the opposite orientation with respect to the dual basis if $n \equiv 2, 3 \mod 4$.

As we have noted, in terms of sewing axioms, if a boundary circle on a topological surface $\Sigma$ of type $(g, n)$ is oriented according to the induced orientation, then this is an *input* circle to which we assign an element of $A$. If a boundary circle is oppositely oriented, then it is an *output* circle and $\Sigma$ produces an output element at this boundary. Thus if $\Sigma_1$ has an input circle and $\Sigma_2$ an output circle, then we can sew the two surfaces together along the circle to form a connected sum $\Sigma_1 \# \Sigma_2$, where the output from $\Sigma_2$ is placed as input for $\Sigma_1$.

**Proposition 3.5.** *The genus* 0 *values of a 2D TQFT is given by*

$$\Omega_{0,n}(v_1, \dots, v_n) = \epsilon(v_1 \cdots v_n), \tag{3.12}$$

*provided that we* define

$$\Omega_{0,3}(v_1, v_2, v_3) := \epsilon(v_1 v_2 v_3). \tag{3.13}$$

*Proof.* This is a direct consequence of CohFT 3 and (2.7). □

One of the original motivations of TQFT [2, 30] is to identify the *topological invariant* $Z(\Sigma)$ of a closed manifold $\Sigma$. In our current setting, it is defined as

$$Z(\Sigma_g) := \epsilon\big(\lambda^{-1}(\Omega_{g,1})\big) \tag{3.14}$$

for a closed oriented surface $\Sigma_g$ of genus $g$. Here, $\Omega_{g,1} : A \longrightarrow K$ is an element of $A^*$, and $\lambda : A \xrightarrow{\sim} A^*$ is the canonical isomorphism.

**Proposition 3.6.** *The topological invariant* $Z(\Sigma_g)$ *of* (3.14) *is given by*

$$Z(\Sigma_g) = \epsilon(\mathbf{e}^g), \tag{3.15}$$

*where* $\mathbf{e}^g \in A$ *represents the* $g$*-th power of the Euler element of* (2.9).

**Lemma 3.7.** *We have*

$$\mathbf{e} := m \circ \delta(1) = \lambda^{-1}(\Omega_{1,1}). \tag{3.16}$$

*Proof.* This follows from

$$\Omega_{1,1}(v) = \sum_{a,b} \Omega_{0,3}(v, e_a, e_b)\eta^{ab} = \sum_{a,b} \eta(v, e_a e_b)\eta^{ab} = \eta(v, \mathbf{e})$$

for every $v \in A$. $\square$

*Proof of Proposition 3.6.* Since the starting case $g = 1$ follows from the above Lemma, we prove the formula by induction, which goes as follows:

$$\begin{aligned}
\Omega_{g,1}(v) &= \sum_{a,b} \Omega_{g-1,3}(v, e_a, e_b)\eta^{ab} \\
&= \sum_{i,j,a,b} \Omega_{0,4}(v, e_a, e_b, e_i)\Omega_{g-1,1}(e_j)\eta^{ab}\eta^{ij} \\
&= \sum_{i,j,a,b} \eta(ve_a e_b, e_i)\Omega_{g-1,1}(e_j)\eta^{ab}\eta^{ij} \\
&= \sum_{i,j} \eta(v\mathbf{e}, e_i)\Omega_{g-1,1}(e_j)\eta^{ij} \\
&= \Omega_{g-1,1}(v\mathbf{e}) \\
&= \Omega_{1,1}(v\mathbf{e}^{g-1}) \\
&= \eta(v\mathbf{e}^{g-1}, \mathbf{e}) = \eta(v, \mathbf{e}^g).
\end{aligned}$$

$\square$

A closed genus $g$ surface is obtained by sewing $g$ genus 1 pieces with one output boundaries to a genus 0 surface with $g$ input boundaries. Since the Euler element is the output of the genus 1 surface with one boundary, we obtain the same result

$$Z(\Sigma_g) = \Omega_{0,g}(\overbrace{\mathbf{e}, \ldots, \mathbf{e}}^{g}).$$

Finally we have the following:

**Theorem 3.8.** *The value or the 2D TQFT is given by*

$$\Omega_{g,n}(v_1, \ldots, v_n) = \epsilon(v_1 \cdots v_n \mathbf{e}^g). \tag{3.17}$$

*Proof.* The argument is the same as the proof of Proposition 3.6:

$$\begin{aligned}
\Omega_{g,n}(v_1, \ldots, v_n) &= \Omega_{1,n}(v_1\mathbf{e}^{g-1}, v_2, \ldots, v_n) \\
&= \sum_{a,b} \Omega_{0,n+2}(v_1\mathbf{e}^{g-1}, v_2, \ldots, v_n, e_a, e_b)\eta^{ab} \\
&= \epsilon(v_1 \cdots v_n \mathbf{e}^g).
\end{aligned}$$

$\square$

**Example 3.9.** Let $G$ be a finite group. The center of the complex group algebra $Z\mathbb{C}[G]$ is a semi-simple Frobenius algebra over $\mathbb{C}$. For every conjugacy class $c$ of $G$, the sum of group elements in $c$,

$$v(C) := \sum_{u \in C} u \in \mathbb{C}[G],$$

is central and defines an element of $Z\mathbb{C}[G]$. Although we do not discuss it any further here, the corresponding TQFT is equivalent to counting problems of character varieties of the fundamental group of $n$-punctured topological surface of genus $g$ into $G$.

## 4. The edge-contraction axioms

In this section we give a formulation of 2D TQFTs based on the edge-contraction operations on cell graphs and a new set of axioms. The main theorem of this section, Theorem 4.7, motivates our construction of the category of cell graphs and the Frobenius ECO functor in Section 5.

**Definition 4.1** (Cell graphs)**.** A connected **cell graph** of topological type $(g, n)$ is the 1-skeleton (the union of 0-cells and 1-cells) of a cell-decomposition of a connected compact oriented topological surface of genus $g$ with $n$ labeled 0-cells. We call a 0-cell a *vertex*, a 1-cell an *edge*, and a 2-cell a *face*, of a cell graph.

**Remark 4.2.** The *dual* of a cell graph is usually referred to as a *ribbon graph*, or a *dessin d'enfant* of Grothendieck. A ribbon graph is a graph with cyclic order assigned to incident half-edges at each vertex. Such assignments induce a cyclic order of half-edges at each vertex of the dual graph. Thus a cell graph itself is a ribbon graph. We note that vertices of a cell graph are labeled, which corresponds to the usual face labeling of a ribbon graph.

**Remark 4.3.** We identify two cell graphs if there is a homeomorphism of the surfaces that brings one cell-decomposition to the other, keeping the labeling of 0-cells. The only possible automorphisms of a cell graph come from cyclic rotations of half-edges at each vertex.

We denote by $\Gamma_{g,n}$ the set of connected cell graphs of type $(g, n)$ with labeled vertices.

**Definition 4.4** (Edge-contraction axioms)**.** The **edge-contraction axioms** are the following set of rules for the assignment

$$\Omega : \Gamma_{g,n} \longrightarrow (A^*)^{\otimes n} \tag{4.1}$$

of a multilinear map

$$\Omega(\gamma) : A^{\otimes n} \longrightarrow K$$

to each cell graph $\gamma \in \Gamma_{g,n}$. We consider $\Omega(\gamma)$ an $n$-variable function $\Omega(\gamma)(v_1, \ldots, v_n)$, where we assign $v_i \in A$ to the $i$-th vertex of $\gamma$.

- **ECA 0**: For the simplest cell graph $\gamma_0 = \bullet \in \Gamma_{0,1}$ that consists of only one vertex without any edges, we define

$$\Omega(\bullet)(v) = \epsilon(v), \qquad v \in A. \tag{4.2}$$

- **ECA 1**: Suppose there is an edge $E$ connecting the $i$-th vertex and the $j$-th vertex for $i < j$ in $\gamma \in \Gamma_{g,n}$. Let $\gamma' \in \Gamma_{g,n-1}$ denote the cell graph obtained by contracting $E$. Then

$$\Omega(\gamma)(v_1, \ldots, v_n) = \Omega(\gamma')(v_1, \ldots, v_{i-1}, v_i v_j, v_{i+1}, \ldots, \widehat{v_j}, \ldots, v_n), \tag{4.3}$$

where $\widehat{v_j}$ means we omit the $j$-th variable $v_j$ at the $j$-th vertex, which no longer exists in $\gamma'$.

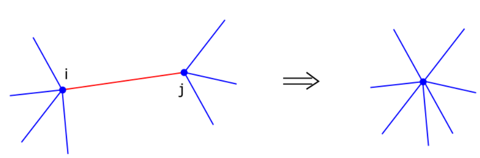


FIGURE 4.1. The edge-contraction operation that shrinks a straight edge connecting Vertex $i$ and Vertex $j$.

- **ECA 2**: Suppose there is a loop $L$ in $\gamma \in \Gamma_{g,n}$ at the $i$-th vertex. Let $\gamma'$ denote the possibly disconnected graph obtained by contracting $L$ and separating the vertex to two distinct vertices labeled by $i$ and $i'$. For the purpose of labeling all vertices, we assign an ordering $i-1 < i < i' < i+1$.

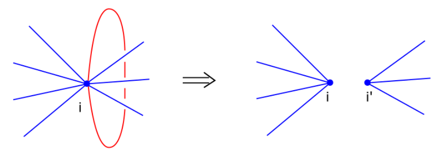


FIGURE 4.2. The edge-contraction operation that shrinks a loop attached Vertex $i$.

If $\gamma'$ is connected, then it is in $\Gamma_{g-1,n+1}$. We call $L$ a *loop of a handle*. We then impose

$$\Omega(\gamma)(v_1,\dots,v_n) = \Omega(\gamma')(v_1,\dots,v_{i-1},\delta(v_i),v_{i+1},\dots,v_n), \tag{4.4}$$

where the outcome of the comultiplication $\delta(v_i)$ is placed in the $i$-th and $i'$-th slots.

If $\gamma'$ is disconnected, then write $\gamma' = (\gamma_1,\gamma_2) \in \Gamma_{g_1,|I|+1} \times \Gamma_{g_2,|J|+1}$, where

$$\begin{cases} g = g_1 + g_2 \\ I \sqcup J = \{1,\dots,\widehat{i},\dots,n\} \end{cases}. \tag{4.5}$$

In this case $L$ is a *separating loop*. Here, vertices labeled by $I$ belong to the connected component of genus $g_1$, and those labeled by $J$ on the other component. Let $(I_-, i, I_+)$ (reps. $(J_-, i, J_+)$) be reordering of $I \sqcup \{i\}$ (resp. $J \sqcup \{i\}$) in the increasing order. We impose

$$\Omega(\gamma)(v_1,\dots,v_n) = \sum_{a,b,k,\ell} \eta(v_i, e_k e_\ell)\eta^{ka}\eta^{\ell b}\Omega(\gamma_1)(v_{I_-}, e_a, v_{I_+})\Omega(\gamma_2)(v_{J_-}, e_b, v_{J_+}), \tag{4.6}$$

which is similar to (4.4), just the comultiplication $\delta(v_i)$ is written in terms of the basis. Here, cocommutativity of $A$ is assumed in this formula.

**Remark 4.5.** We do not assume the permutation symmetry of $\Omega(\gamma)(v_1,\dots,v_n)$. The cumbersome notation of the axioms is due to keeping track of the ordering of indices.

**Remark 4.6.** Let us define $m(\gamma) = 2g-2+n$ for $\gamma \in \Gamma_{g,n}$. The edge-contraction operations are reduction of $m(\gamma)$ exactly by 1. Indeed, for ECA 1, we have

$$m(\gamma') = 2g - 2 + (n-1) = m(\gamma) - 1.$$

ECA 2 applied to a loop of a handle produces

$$m(\gamma') = 2(g-1) - 2 + (n+1) = m(\gamma) - 1.$$

For a separating loop, we have

$$\begin{array}{rc} & 2g_1 - 2 + |I| + 1 \\ +) & 2g_2 - 2 + |J| + 1 \\ \hline & 2g_1 + 2g_2 - 4 + |I| + |J| + 2 \end{array} \;=\; 2g - 2 + n - 1.$$

This reduction is used in the proof of the following theorem.

**Theorem 4.7** (Graph independence)**.** *As the consequence of the edge-contraction axioms, every connected cell graph $\gamma \in \Gamma_{g,n}$ gives rise to the same map*

$$\Omega(\gamma) : A^{\otimes n} \ni v_1 \otimes \cdots \otimes v_n \longmapsto \epsilon(v_1 \cdots v_n \mathbf{e}^g) \in K, \tag{4.7}$$

*where* $\mathbf{e}$ *is the Euler element of* (2.9)*. In particular,* $\Omega(\gamma)(v_1, \ldots, v_n)$ *is symmetric with respect to permutations of indices.*

**Corollary 4.8** (ECA implies TQFT)**.** *Define* $\Omega_{g,n}(v_1, \ldots, v_n) = \Omega(\gamma)(v_1, \ldots, v_n)$ *for any* $\gamma \in \Gamma_{g,n}$*. Then* $\{\Omega_{g,n}\}$ *is the 2D TQFT associated with the Frobenius algebra $A$. Every 2D TQFT is obtained in this way, hence the two descriptions of 2D TQFT are equivalent.*

*Proof of Corollary 4.8 assuming Theorem 4.7.* Since both ECAs and 2D TQFT give the unique value

$$\Omega(\gamma)(v_1, \ldots, v_n) = \epsilon(v_1 \cdots v_n \mathbf{e}^g) = \Omega_{g,n}(v_1, \ldots, v_n)$$

for all $(g, n)$ from (3.17), we see that the two sets of axioms are equivalent, and also that the edge-contraction axioms produce evert 2D TQFT. ☐

To illustrate the graph independence, let us first examine three simple cases.

**Lemma 4.9** (Edge-removal lemma)**.** *Let* $\gamma \in \Gamma_{g,n}$*.*

(1) *Suppose there is a disc-bounding loop $L$ in $\gamma$ (the graph on the left of Figure 4.3). Let $\gamma' \in \Gamma_{g,n}$ be the graph obtained by removing $L$ from $\gamma$.*
(2) *Suppose there are two edges $E_1$ and $E_2$ between two distinct vertices Vertex $i$ and Vertex $j$, $i < j$, that bound a disc (the middle graph of Figure 4.3). Let $\gamma' \in \Gamma_{g,n}$ be the graph obtained by removing $E_2$.*
(3) *Suppose two loops, $L_1$ and $L_2$, are attached to the $i$-th vertex (the graph on the right of Figure 4.3). If they are homotopic, then let $\gamma' \in \Gamma_{g,n}$ be the graph obtained by removing $L_2$ from $\gamma$.*

*In each of the above cases, we have*

$$\Omega(\gamma)(v_1, \ldots, v_n) = \Omega(\gamma')(v_1, \ldots, v_n). \tag{4.8}$$

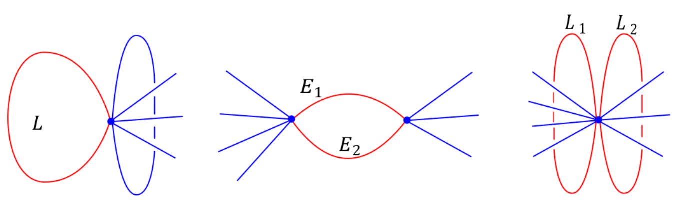


FIGURE 4.3.

*Proof.* (1) Contracting a disc-bounding loop attached to the $i$-th vertex creates $(\gamma_0, \gamma') \in \Gamma_{0,1} \times \Gamma_{g,n}$, where $\gamma_0$ consists of only one vertex and no edges. Then ECA 2 reads

$$\begin{aligned}
\Omega(\gamma)(v_1, \ldots, v_n) &= \sum_{a,b,k,\ell} \eta(v_i, e_k e_\ell)\eta^{ka}\eta^{\ell b}\gamma_0(e_a)\Omega(\gamma')(v_1, \ldots, v_{i-1}, e_b, v_{i+1} \ldots, v_n) \\
&= \sum_{a,b,k,\ell} \eta(v_i, e_k e_\ell)\eta^{ka}\eta^{\ell b}\eta(1, e_a)\Omega(\gamma')(v_1, \ldots, v_{i-1}, e_b, v_{i+1} \ldots, v_n) \\
&= \sum_{b,k,\ell} \eta(v_i, e_k e_\ell)\delta_1^k \eta^{\ell b}\Omega(\gamma')(v_1, \ldots, v_{i-1}, e_b, v_{i+1} \ldots, v_n)
\end{aligned}$$

$$
\begin{aligned}
&= \sum_{b,\ell} \eta(v_i, e_\ell)\eta^{\ell b}\Omega(\gamma')(v_1, \dots, v_{i-1}, e_b, v_{i+1} \dots, v_n) \\
&= \Omega(\gamma')(v_1, \dots, v_{i-1}, v_i, v_{i+1} \dots, v_n).
\end{aligned}
$$

(2) Contracting Edge $E_1$ makes $E_2$ a disc-bounding loop at Vertex $i$. We can remove it by (1). Note that the new Vertex $i$ is assigned with $v_i v_j$. Restoring $E_1$ makes the graph exactly the one obtained by removing $E_2$ from $\gamma$. Thus (4.8) holds.

(3) Contracting Loop $L_1$ makes $L_2$ a disc-bounding loop. Hence we can remove it by (1). Then restoring $L_1$ creates a graph obtained from $\gamma$ by removing $L_2$. Thus (4.8) holds. $\square$

**Remark 4.10.** The three cases treated above correspond to eliminating degree 1 and 2 vertices from the ribbon graph dual to the cell graph. In combinatorial moduli theory, we normally consider ribbon graphs that have no vertices of degree less than 3 [24].

**Definition 4.11** (Reduced graph)**.** We call a cell graph **reduced** if it does not have any disc-bounding loops or disc-bounding bigons. In other words, the dual ribbon graph of a reduced cell graph has no vertices of degree 1 or 2.

We can see from Lemma 4.9 (1) that every $\gamma_{0,1} \in \Gamma_{0,1}$ gives rise to the same map

$$\Omega(\gamma_{0,1})(v) = \epsilon(v). \tag{4.9}$$

Likewise, Lemma 4.9 (1) and (2) show that every $\gamma_{0,2} \in \Gamma_{0,2}$ gives the same map

$$\Omega(\gamma_{0,2})(v_1, v_2) = \eta(v_1, v_2).$$

This is because we can remove all edges and loops but one that connects the two vertices, and from ECA 1, the value of the assignment is $\epsilon(v_1 v_2)$.

*Proof of Theorem 4.7.* We use the induction on $m = 2g - 2 + n$. The base case is $m = -1$, or $(g, n) = (0, 1)$, for which the theorem holds by (4.9). Assume that (4.7) holds for all $(g, n)$ with $2g - 2 + n < m$. Now let $\gamma \in \Gamma_{g,n}$ be a cell graph of type $(g, n)$ such that $2n - 2 + n = m$.

Choose an arbitrary straight edge of $\gamma$ that connects two distinct vertices, say Vertex $i$ and Vertex $j$, $i < j$. By contracting this edge, we obtain by ECA 1,

$$\Omega(\gamma)(v_1, \dots, v_n) = \Omega(\gamma_{g,n-1})(v_1, \dots, v_{i-1}, v_i v_j, v_{i+1} \dots, \widehat{v_j}, \dots, v_n) = \epsilon(v_1 \dots v_n \mathbf{e}^g).$$

If we have chosen an arbitrary loop attached to Vertex $i$, then its contraction by ECA 2 gives two cases, depending on whether the loop is a loop of a handle, or a separating loop. For the first case, by appealing to (2.7) and (2.10), we obtain

$$
\begin{aligned}
\Omega(\gamma)(v_1, \dots, v_n) &= \sum_{a,b,k,\ell} \eta(v_i, e_k e_\ell)\eta^{ka}\eta^{\ell b}\Omega(\gamma_{g-1,n+1})(v_1, \dots, v_{i-1}, e_a, e_b, v_{i+1}, \dots, v_n) \\
&= \sum_{a,b,k,\ell} \eta(v_i e_k, e_\ell)\eta^{ka}\eta^{\ell b}\Omega(\gamma_{g-1,n+1})(v_1, \dots, v_{i-1}, e_a, e_b, v_{i+1}, \dots, v_n) \\
&= \sum_{a,k} \eta^{ka}\Omega(\gamma_{g-1,n+1})(v_1, \dots, v_{i-1}, e_a, v_i e_k, v_{i+1}, \dots, v_n) \\
&= \sum_{a,k} \eta^{ka}\epsilon(v_1 \cdots v_n \mathbf{e}^{g-1} e_a e_b) \\
&= \epsilon(v_1 \cdots v_n \mathbf{e}^g).
\end{aligned}
$$

For the case of a separating loop, again by appealing to (2.7), we have

$$\begin{aligned}
\Omega(\gamma)(v_1,\dots,v_n) &= \sum_{a,b,k,\ell} \eta(v_i, e_k e_\ell)\eta^{ka}\eta^{\ell b}\Omega(\gamma_{g_1,|I|+1})(v_{I_-}, e_a, v_{I_+})\Omega(\gamma_{g_2,|J|+1})(v_{J_-}, e_b, v_{J_+}) \\
&= \sum_{a,b,k,\ell} \eta(v_i, e_k e_\ell)\eta^{ka}\eta^{\ell b}\epsilon\left(e_a \prod_{c\in I} v_c \mathbf{e}^{g_1}\right)\epsilon\left(e_b \prod_{d\in J} v_d \mathbf{e}^{g_2}\right) \\
&= \sum_{a,b,k,\ell} \eta(v_i e_k, e_\ell)\eta^{ka}\eta^{\ell b}\eta\left(\prod_{c\in I} v_c, e_a \mathbf{e}^{g_1}\right)\epsilon\left(e_b \prod_{d\in J} v_d \mathbf{e}^{g_2}\right) \\
&= \sum_{a,k} \eta^{ka}\eta\left(\prod_{c\in I} v_c \mathbf{e}^{g_1}, e_a\right)\epsilon\left(v_i e_k \prod_{d\in J} v_d \mathbf{e}^{g_2}\right) \\
&= \epsilon\left(v_i \prod_{c\in I} v_c \mathbf{e}^{g_1} \prod_{d\in J} v_d \mathbf{e}^{g_2}\right) \\
&= \epsilon(v_1 \cdots v_n \mathbf{e}^{g_1+g_2}).
\end{aligned}$$

Therefore, no matter how we apply ECA 1 or ECA 2, we always obtain the same result. This completes the proof. ☐

**Remark 4.12.** There is a different proof of the graph independence theorem, using a topological idea of deforming graphs similar to the one used in [**?**].

As we see, the key reason for the graph independence of Theorem 4.7 is the property of the Frobenius algebra $A$ that we have, namely, commutativity, cocommutativity, associativity, coassociativity, and the Frobenius relation (2.1). These properties are manifest in the following graph operations. Although the next proposition is an easy consequence of Theorem 4.7, we derive it directly from the ECAs so that we can see how the algebraic structure of the Frobenius algebra is encoded into the TQFT. Indeed, the graph-independence theorem also follows from Proposition 4.13. This fact motivates us to introduce the category of cell graphs and the Frobenius ECO functor in the next section.

**Proposition 4.13** (Commutativity of Edge Contractions)**.** *Let $\gamma \in \Gamma_{g,n}$.*

(1) *Suppose Vertex $i$ is connected to two distinct vertices Vertex $j$ and Vertex $k$ by two edges, $E_j$ and $E_k$. The graph we obtain, denoted as $\gamma' \in \Gamma_{g,n-2}$, by first contracting $E_j$ and then contracting $E_k$, is the same as contracting the edges in the opposite order. The two different orders of the application of ECA 1 then gives the same answer. For example, if $i < j < k$, then we have*

$$\Omega(\gamma)(v_1,\dots,v_n) = \Omega(\gamma')(v_1,\dots,v_{i-1}, v_i v_j v_k, v_{i+1},\dots,\widehat{v_j},\dots,\widehat{v_k},\dots,v_n). \tag{4.10}$$

(2) *Suppose two loops $L_1$ and $L_2$ are connected to Vertex $i$. Then the contraction of the two loops in different orders gives the same result.*

(3) *Suppose a loop $L$ and a straight edge $E$ are attached to Vertex $i$, where $E$ connects to Vertex $j$, $i \neq j$. Then contracting $L$ first and followed by contracting $E$, gives the same result as we contract $L$ and $E$ in the other way around.*

*Proof.* (1) There are three possible cases: $i < j < k$, $j < i < k$, and $j < k < i$. In each case, the result is replacing $v_i$ by $v_i v_j v_k$, and removing two vertices. The associativity and commutativity of the multiplication of $A$ make the result of different contractions the same.

(2) There are two cases here: After the contraction of one of the loops, (a) the other loop remans to be a loop, or (b) becomes an edge connecting the two vertices created by the contraction of the first loop.

In the first case (a), the contraction of the two loops makes Vertex $i$ in $\gamma$ into three different vertices $i_1, i_2, i_3$ of the resulting graph $\gamma'$, which may be disconnected. The loop contractions in the two different orders produce triple tensor products

$$(1 \otimes \delta)\delta(v_i) = (\delta \otimes 1)\delta(v_i),$$

which are equal by the coassociativity

$$\begin{tikzcd} & A \otimes A \arrow[dr, "1\otimes\delta"] & \\ A \arrow[ur, "\delta"] \arrow[dr, "\delta"'] & & A \otimes A \otimes A. \\ & A \otimes A \arrow[ur, "\delta\otimes 1"'] & \end{tikzcd}$$

For (b), the contraction of the loops in either order will produce $m \circ \delta(v_i)$ on the same $i$-th slot of the same graph $\gamma' \in \Gamma_{g-1,n}$.

(3) This amounts to proving the equation

$$\delta(v_i v_j) = (1 \otimes m)\big(\delta(v_i), v_j\big) = (m \otimes 1)\big(v_j, \delta(v_i)\big),$$

which is Lemma 2.1. $\square$

**Remark 4.14.** If we have a system of subsets $\Gamma'_{g,n} \subset \Gamma_{g,n}$ for all $(g, n)$ that is closed under the edge-contraction operations, then all statements of this section still hold by replacing $\Gamma_{g,n}$ by $\Gamma'_{g,n}$.

**Remark 4.15.** Chen [6] proved the graph independence for a special case of $A = Z\mathbb{C}[S_3]$, the center of the group algebra for symmetric group $S_3$, by direct computation. This result led the authors to find a general proof of Theorem 4.7.

The edge-contraction operations are associated with gluing morphisms of $\overline{\mathcal{M}}_{g,n}$ that are different from those in (3.4) and (3.5). ECA 1 of (4.3) is associated with

$$\alpha : \overline{\mathcal{M}}_{0,3} \times \overline{\mathcal{M}}_{g,n-1} \longrightarrow \overline{\mathcal{M}}_{g,n}. \tag{4.11}$$

The handle cutting case of ECA 2 of (4.4) is associated with

$$\beta_1 : \overline{\mathcal{M}}_{0,3} \times \overline{\mathcal{M}}_{g-1,n+1} \longrightarrow \overline{\mathcal{M}}_{g,n}, \tag{4.12}$$

and the separating loop contraction with

$$\beta_2 : \overline{\mathcal{M}}_{0,3} \times \overline{\mathcal{M}}_{g_1,|I|+1} \times \overline{\mathcal{M}}_{g_2,|J|+1} \longrightarrow \overline{\mathcal{M}}_{g_1+g_2,|I|+|J|+1}. \tag{4.13}$$

Although there are no cell graph operations that are directly associated with the forgetful morphism $\pi$ and the gluing maps $gl_1$ and $gl_2$, there is an operation on cell graphs similar to the *connected sum* of topological surfaces.

**Definition 4.16** (Connected sum of cell graphs)**.** Let $\gamma'$ be a cell graph with the following conditions.

(1) There is a vertex $q$ in $\gamma'$ of degree $d$.
(2) There are $d$ distinct edges incident to $q$. In particular, none of them is a loop.
(3) There are exactly $d$ faces in $\gamma'$ incident to $q$.

Given an arbitrary cell graph $\gamma$ with a degree $d$ vertex $p$, we can create a new cell graph $\gamma\#_{(p,q)}\gamma'$, which we call the *connected sum* of $\gamma$ and $\gamma'$. The procedure is the following. We label all half-edges incident to $p$ with $\{1,2,\dots,d\}$ according to the cyclic order of the cell graph $\gamma$ at $p$. We also label all edges incident to $q$ in $\gamma'$ with $\{1,2,\dots,d\}$, but this time opposite to the cyclic oder given to $\gamma'$ at $q$. Cut a small disc around $p$ and $q$, and connect all half-edges according to the labeling. The result is a cell graph $\gamma\#_{(p,q)}\gamma'$.

**Remark 4.17.** The connected sum construction can be applied to two distinct vertices $p$ and $q$ of the same graph, provided that these vertices satisfy the required conditions.

**Remark 4.18.** The total number of vertices decreases by 2 in the connected sum. Therefore, two 1-vertex graphs cannot be connected by this construction.

The connected sum construction provides the inverse of the edge-contraction operations as the following diagrams show. It is also clear from these figures that the edge-contraction operations are degeneration of curves producing a rational curve with three special points, as indicated in Introduction.

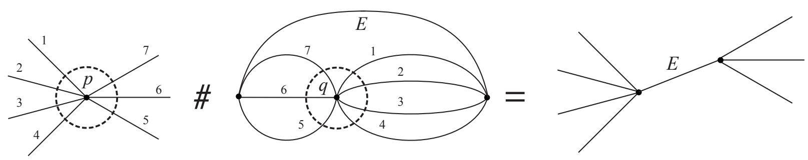


FIGURE 4.4. The connected sum of a cell graph with a particular type $(0,3)$ cell graph gives the inverse of the edge-contraction operation on $E$ that connects two distinct vertices. The connected sum with the $(0,3)$ piece has to be done so that the edges incidents on each side of $E$ match the original graph.

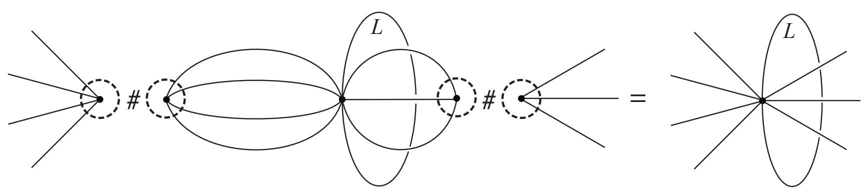


FIGURE 4.5. The edge-contraction operation on a loop $L$ is the inverse of two connected sum operations, with a type $(0,3)$ piece in the middle.

## 5. Category of cell graphs and Frobenius ECO functors

In the previous section, we started from a Frobenius algebra $A$ and constructed the corresponding TQFT through edge-contraction axioms. The key step is the assignment of the linear map $\Omega(\gamma) : A^{\otimes n} \longrightarrow K$ to each cell graph $\gamma \in \Gamma_{g,n}$. As we have noticed, edge-contraction operations encode the structure of a Frobenius algebra. These considerations suggest that cell graphs are functors, and edge-contraction operations are natural transformations. In this section, we define the category of cell graphs, and define Frobenius ECO functors, which make edge-contraction operations correspond to natural transformations.

Let $(\mathcal{C},\otimes,K)$ be a monoidal category with a bifunctor $\otimes : \mathcal{C}\times\mathcal{C} \longrightarrow \mathcal{C}$ and its left and right identity object $K \in Ob(\mathcal{C})$. The example we keep in mind is the monoidal category $(\mathbf{Vect},\otimes,K)$ of vector spaces defined over a field $K$ with the vector space tensor product operation. Fore brevity, we call the bifunctor $\otimes$ just as a tensor product. A $K$-object in $\mathcal{C}$ is a pair $(V, f : V \longrightarrow K)$ consisting of an object $V$ and a morphism $f : V \longrightarrow K$. We denote by $\mathcal{C}/K$ the category of $K$-objects in $\mathcal{C}$. A $K$-morphism $h : (V_1, f_1) \longrightarrow (V_2, f_2)$ is a morphism $h : V_1 \longrightarrow V_2$ in $\mathcal{C}$ that satisfies the commutativity

$$\begin{tikzcd} V_1 \arrow[r, "f_1"] \arrow[d, "h"'] & K \arrow[d, equal] \\ V_2 \arrow[r, "f_2"'] & K \end{tikzcd}. \tag{5.1}$$

We note that every morphism $h : V_1 \longrightarrow V_2$ in $\mathcal{C}$ yields a new object $(V_1, f_1)$ from a given $(V_2, f_2)$ as in (5.1). This is the *pull-back* object. The category $\mathcal{C}/K$ itself is a monoidal category with respect to the tensor product, and the final object $(K, id_K : K \longrightarrow K)$ of $\mathcal{C}/K$ as its identity object.

We denote by $\mathcal{F}un(\mathcal{C}/K, \mathcal{C}/K)$ the **endofunctor category**, consisting of monoidal functors

$$\alpha : \mathcal{C}/K \longrightarrow \mathcal{C}/K$$

as its objects. Let $\alpha$ and $\beta$ be two endofunctors, and $\tau$ a natural transformation between them. Natural transformations form morphisms in the endofunctor category.

$$\begin{tikzcd} V \arrow[dr, "f"] \arrow[dd, "h"'] & \\ & K \\ W \arrow[ur, "g"'] & \end{tikzcd} \qquad \begin{tikzcd} \alpha(V) \arrow[rr, "\tau"] \arrow[dr, "\alpha(f)"] \arrow[dd, "\alpha(h)"'] & & \beta(V) \arrow[dr, "\beta(f)"] \arrow[dd] & \\ & K \arrow[rr, "\tau"] & & K \\ \alpha(W) \arrow[rr, "\tau"'] \arrow[ur, "\alpha(g)"'] & & \beta(W) \arrow[ur, "\beta(g)"'] & \end{tikzcd}$$

The final object of $\mathcal{F}un(\mathcal{C}/K, \mathcal{C}/K)$ is the functor

$$\phi : (V, f : V \longrightarrow K) \longrightarrow (K, id_K : K \longrightarrow K) \tag{5.2}$$

which assigns the final object of the codomain $\mathcal{C}/K$ to everything in the domain $\mathcal{C}/K$. With respect to the tensor product and the above functor $\phi$ as its identity object, the endofunctor category $\mathcal{F}un(\mathcal{C}/K, \mathcal{C}/K)$ is again a monoidal category.

**Definition 5.1** (Subcategory generated by $V$)**.** For every choice of an object $V$ of $\mathcal{C}$, we define a category of $K$-objects $\mathcal{T}(V^\bullet)/K$ as the full subcategory of $\mathcal{C}/K$ whose objects are $(V^{\otimes n}, f : V^{\otimes n} \longrightarrow K)$, $n = 0, 1, 2, \dots$. We call $\mathcal{T}(V^\bullet)/K$ the **subcategory generated by** $V$ **in** $\mathcal{C}/K$.

**Definition 5.2** (Monoidal category of cell graphs)**.** The finite coproduct (or cocartesian) **monoidal category of cell graphs** $\mathcal{CG}$ is defined as follows.

- The set of objects $Ob(\mathcal{CG})$ consists of a finite disjoint union of cell graphs.
- The coproduct in $\mathcal{CG}$ is the disjoin union, and the coidentity object is the empty graph.

The set of morphism $\text{Hom}(\gamma_1, \gamma_2)$ from a cell graph $\gamma_1$ to $\gamma_2$ consists of equivalence classes of sequences of edge-contraction operations and graph automorphisms. For brevity of notation, if $E$ is an edge connecting two distinct vertices of $\gamma_1$, then we simply denote by $E$ itself as the edge-contraction operation shrinking $E$, as in Figure 4.1. If $L$ is a loop in $\gamma_1$, then we denote by $L$ the edge-contraction operation of Figure 4.2. Let

$$\widetilde{\mathrm{Hom}}(\gamma_1,\gamma_2) = \left\{ \begin{array}{c} \text{composition of a sequence of edge-contractions} \\ \text{and graph automorphisms that changes } \gamma_1 \text{ to } \gamma_2 \end{array} \right\}.$$

This is the set of words consisting of edge-contraction operations and graph automorphisms that change $\gamma_1$ to $\gamma_2$ when operated consecutively. If there is no such operations, then we define $\widetilde{\mathrm{Hom}}(\gamma_1,\gamma_2)$ to be the empty set. The morphism set $\mathrm{Hom}(\gamma_1,\gamma_2)$ is the set of equivalence classes of $\widetilde{\mathrm{Hom}}(\gamma_1,\gamma_2)$. The equivalence relation in the extended morphism set is generated by the following cases of equivalences.

(1) Suppose $\gamma_1$ has a non-trivial automorphism $\sigma$. Then for every edge $E$ of $\gamma_1$, $E$ and $\sigma(E)$ are equivalent.
(2) Suppose Vertex $i$ of $\gamma_1 \in \Gamma_{g,n}$ is connected to two distinct vertices Vertex $j$ and Vertex $k$ by two edges, $E_j$ and $E_k$. The graph we obtain, denoted as $\gamma_2 \in \Gamma_{g,n-2}$, by first contracting $E_j$ and then contracting $E_k$, is the same as contracting the edges in the opposite order. The two words $E_1E_2$ and $E_2E_1$ are equivalent.
(3) Suppose two loops $L_1$ and $L_2$ of $\gamma_1$ are connected to Vertex $i$. Then the contraction operations of the two loops in different orders give the same result. The two words $L_1L_2$ and $L_2L_1$ are equivalent.
(4) Suppose a loop $L$ and a straight edge $E$ in $\gamma_1$ are attached to Vertex $i$, where $E$ connects to Vertex $j$, $i \neq j$. Then contracting $L$ first and followed by contracting $E$, gives the same result as we contract $L$ and $E$ in the other way around. The two words $EL$ and $LE$ are equivalent.
(5) Suppose $\gamma_1$ has two edges (including loops) $E_1$ and $E_2$ that have no common vertices, and $\gamma_2$ is obtained by contracting them. Then $E_1E_2$ is equivalent to $E_2E_1$.
(6) Suppose two edges $E_1$ and $E_2$ are both incident to two distinct vertices. Then $E_1E_2$ is equivalent to $E_2E_1$.

**Example 5.3.** A few simple examples of morphisms are given below.

$$\mathrm{Hom}(\bullet\overset{E_1}{-\!\!-\!\!-}\bullet\overset{E_2}{-\!\!-\!\!-}\bullet, \bullet\!-\!\!-\!\!-\!\bullet) = \{E_1, E_2\},$$

$$\mathrm{Hom}(\bullet\overset{E_1}{-\!\!-\!\!-}\bullet\overset{E_2}{-\!\!-\!\!-}\bullet, \bullet) = \{E_1E_2\},$$

$$\mathrm{Hom}\left(\bullet\!\overset{E_1}{\underset{E_2}{\bigcirc}}\!\bullet, \bullet\!\bigcirc\right) = \{E_1\} = \{\sigma(E_1)\} = \{E_2\},$$

$$\mathrm{Hom}\left(\bullet\!\overset{E_1}{\underset{E_2}{\bigcirc}}\!\bullet, \bullet \quad \bullet\right) = \{E_1E_2\}.$$

The cell graph on the left of the third and fourth lines has an automorphism $\sigma$ that interchanges $E_1$ and $E_2$. Thus as the edge-contraction operation, $E_2 = E_1 \circ \sigma = \sigma(E_1)$.

**Remark 5.4.** If $\gamma \in \Gamma_{g,n}$, then $\mathrm{Hom}(\gamma,\gamma) = \{id_\gamma\}$.

We have seen in the last section that when we have made a choice of a unital commutative Frobenius algebra $A$, a cell graph $\gamma \in \Gamma_{g,n}$ defines a multilinear map $\Omega_A(\gamma) : A^{\otimes n} \longrightarrow K$ subject to edge-contraction axioms. For a different Frobenius algebra $B$, we have a different multilinear map $\Omega_B(\gamma) : B^{\otimes n} \longrightarrow K$, subject to the same axioms. These two maps are unrelated, unless we have a Frobenius algebra homomorphism $h : A \longrightarrow B$. Theorem 4.7

tells us that we have a $K$-morphism of (5.1) which induces $\Omega_A(\gamma)$ as the pull-back of $\Omega_B(\gamma)$.

$$\begin{tikzcd} A \arrow[d, "h"'] & A^{\otimes n} \arrow[r, "\Omega_A(\gamma)"] \arrow[d] & K \arrow[d] \\ B & B^{\otimes n} \arrow[r, "\Omega_B(\gamma)"'] & K \end{tikzcd}$$

This consideration suggests that $\Omega(\gamma)$ is a functor defined on the category of Frobenius algebras. But since we are encoding the Frobenius algebra structure into the category of cell graphs, the extra choice of Frobenius algebras is redundant.

We are thus led to the following definition.

**Definition 5.5** (Frobenius ECO functor)**.** An **Frobenius ECO functor** is a monoidal functor

$$\omega : \mathcal{CG} \longrightarrow \mathcal{F}un(\mathcal{C}/K, \mathcal{C}/K) \tag{5.3}$$

satisfying the following conditions.

- The graph $\gamma_0 = \bullet$ of (4.2) of type $(0,1)$ consisting of only one vertex and no edges corresponds to the identity endofunctor:

$$\bullet \longrightarrow (id : \mathcal{C}/K \longrightarrow \mathcal{C}/K). \tag{5.4}$$

- A graph $\gamma \in \Gamma_{g,n}$ of type $(g,n)$ corresponds to a functor

$$\gamma \longmapsto \left[(V, f : V \longrightarrow K) \longrightarrow (V^{\otimes n}, \omega_V(\gamma) : V^{\otimes n} \longrightarrow K)\right]. \tag{5.5}$$

The Frobenius ECO functor assigns to each edge-contraction operation a natural transformation of endofunctors $\mathcal{C}/K \longrightarrow \mathcal{C}/K$.

**Remark 5.6.** The unique construction of the Frobenius ECO functor for $(\mathbf{Vect}, \otimes, K)$ requires us to generalize our categorical setting to include CohFT of Kontsevich-Manin [21]. Then we will be able to show that this unique functor actually generates all *Frobenius objects* of $(\mathbf{Vect}, \otimes, K)$. This topic will be treated in our forthcoming paper.

Let us consider the monoidal (not full) subcategory $\mathcal{A} \subset (\mathbf{Vect}, \otimes, K)$ consisting of commutative and cocommutative Frobenius algebras.

**Theorem 5.7** (Construction of 2D TQFTs)**.** *There is a canonical Frobenius ECO functor*

$$\Omega : \mathcal{CG} \longrightarrow \mathcal{F}un(\mathcal{A}/K, \mathcal{A}/K). \tag{5.6}$$

*When we start with a Frobenius algebra $A$, this functor generates a network of multilinear maps*

$$\Omega_A(\gamma) : A^{\otimes n} \longrightarrow K$$

*for all cell graphs $\gamma \in \Gamma_{g,n}$ for all values of $(g,n)$. This is the 2D TQFT corresponding to the Frobenius algebra $A$.*

*Proof.* This follows from the graph independence of Theorem 4.7. $\square$

## 6. Orbifold Hurwitz numbers as graph enumeration

Mirror symmetry provides an effective tool for counting problems of Gromov-Witten type invariants. The question is how we construct the mirror, given a counting problem. Although there is so far no general formalism, we present a systematic procedure for computing orbifold Hurwitz numbers in this second part of the paper. The key observation is that the edge-contraction operations for $(g, n) = (0, 1)$ identify the mirror object.

The topological recursion for simple and orbifold Hurwitz numbers are derived as the Laplace transform of the cut-and-join equation [4, 14, 27], where the spectral curves are identified by the consideration of mirror symmetry of toric Calabi-Yau orbifolds [4, 5]. In this section we give a purely combinatorial graph enumeration problem that is equivalent to counting orbifold Hurwitz numbers. We then show in the next section that the edge-contraction formula restricted to the $(g, n) = (0, 1)$ case determines the spectral curve and the differential forms $W_{0,1}$ and $W_{0,2}$ of [4]. These quantities form the mirror objects for the orbifold Hurwitz numbers.

### 6.1. $r$-Hurwitz graphs.

We choose and fix a positive integer $r$. The decorated graphs we wish to enumerate are the following.

**Definition 6.1** ($r$-Hurwitz graph)**.** An $r$-**Hurwitz graph** $(\gamma, D)$ of type $(g, n, d)$ consists of the following data.

- $\gamma$ is a connected cell graph of type $(g, n)$, with $n$ labeled vertices as in earlier sections.
- $|D| = d$ is divisible by $r$, and $\gamma$ has $m = d/r$ unlabeled faces and $s$ unlabeled edges, where

$$s = 2g - 2 + \frac{d}{r} + n. \tag{6.1}$$

- $D$ is a configuration of $d = rm$ unlabeled dots on the graph subject to the following conditions:
  (1) The set of $d$ dots are grouped into $m$ subsets of $r$ dots, each of which is equipped with a cyclic order.
  (2) Every face of $\gamma$ has cyclically ordered $r$ dots.
  (3) These dots are clustered near vertices of the face. At each corner of the face, say at Vertex $i$, the dots are ordered according to the cyclic order that is consistent of the orientation of the face, which is chosen to be counter-clock wise.
  (4) Let $\mu_i$ denote the total number of dots clustered at Vertex $i$. Then $\mu_i > 0$ for every $i = 1, \dots, n$. Thus we have an ordered partition

$$d = \mu_1 + \cdots + \mu_n. \tag{6.2}$$

  In particular, the number of vertices ranges $0 < n \leq d$.
  (5) Suppose an edge $E$ connecting two distinct vertices, say Vertex $i$ and $j$, bounds the same face twice. Let $p$ be the midpoint of $E$. The polygon representing the face has $E$ twice on its perimeter, hence the point $p$ appears also twice. We name them as $p$ and $p'$. Which one we call $p$ or $p'$ does not matter. Consider a path on the perimeter of this polygon starting from $p$ and ending up with $p'$ according to the counter-clock wise orientation. Let $r'$ be the total number of dots clustered around vertices of the face, counted along the path. Then it satisfies

$$0 < r' < r. \tag{6.3}$$

For example, not all $r$ dots of a face can be clustered at a vertex of degree 1. In particular, for the case of $r = 1$, the graph $\gamma$ has no edges bounding the same face twice.

An **arrowed** $r$-Hurwitz graph $(\gamma, \vec{D})$ has, in addition to to the above data $(\gamma, D)$, an arrow assigned to one of the $\mu_i$ dots from Vertex $i$ for each index $1 \le i \le n$.

The counting problem we wish to study is the number $\mathcal{H}^r_{g,n}(\mu_1 \dots, \mu_n)$ of arrowed $r$-Hurwitz graphs for a prescribed ordered partition (6.2), counted with the automorphism weight. The combinatorial data corresponds to an object in algebraic geometry. Let us first identify what the $r$-Hurwitz graphs represent. We denote by $\mathbb{P}^1[r]$ the 1-dimensional orbifold modeled on $\mathbb{P}^1$ that has one stacky point $\big[0/\big(\mathbb{Z}/(r)\big)\big]$ at $0 \in \mathbb{P}^1$.

**Example 6.2.** The base case is $\mathcal{H}^r_{0,1}(r) = 1$ (see Figure 6.1). This counts the identity morphism $\mathbb{P}^1[r] \xrightarrow{\sim} \mathbb{P}^1[r]$.

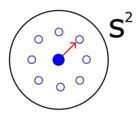


FIGURE 6.1. The graph has only one vertex and no edges. All $r$ dots are clustered around this unique vertex, with an arrow attached to one of them. Because of the arrow, there is no automorphism of this graph.

**Definition 6.3** (Orbifold Hurwitz cover and Orbifold Hurwitz numbers)**.** An *orbifold Hurwitz cover* $f : C \longrightarrow \mathbb{P}^1[r]$ is a morphism from an orbifold $C$ that is modeled on a smooth algebraic curve of genus $g$ that has

(1) $m$ stacky points of the same type as the one on the base curve that are all mapped to $\big[0/\big(\mathbb{Z}/(r)\big)\big] \in \mathbb{P}^1[r]$,
(2) arbitrary profile $(\mu_1, \dots, \mu_n)$ with $n$ labeled points over $\infty \in \mathbb{P}^1[r]$,
(3) and all other ramification points are simple.

If we replace the target orbifold by $\mathbb{P}^1$, then the morphism is a regular map from a smooth curve of genus $g$ with profile $(\overbrace{r, \dots, r}^{m})$ over $0 \in \mathbb{P}^1$, labeled profile $(\mu_1, \dots, \mu_n)$ over $\infty \in \mathbb{P}^1$, and a simple ramification at any other ramification point. The Euler characteristic condition (6.1) of the graph $\gamma$ gives the number of simple ramification points of $f$ through the Riemann-Hurwitz formula. The automorphism weighted count of the number of the topological types of such covers is denoted by $H^r_{g,n}(\mu_1, \dots, \mu_n)$. These numbers are referred to as *orbifold Hurwitz numbers*. When $r = 1$, they count the usual simple Hurwitz numbers.

The counting of the topological types is the same as counting actual orbifold Hurwitz covers such that all simple ramification points are mapped to one of the $s$-th roots of unity $\xi^1, \dots, \xi^s$, where $\xi = \exp(2\pi i/s)$, if all simple ramification points of $f$ are labeled. Indeed, such a labeling is given by elements of the cyclic group $\{\xi^1, \dots, \xi^s\}$ of order $s$. Let us construct an edge-labeled Hurwitz graph from an orbifold Hurwitz cover with fixed branch points on the target as above. We first review the case of $r = 1$, i.e., the simple Hurwitz covers. Our graph is essentially the same as the dual of the *branching graph* of [29].

6.2. **Construction of Hurwitz graphs for $r = 1$.** Let $f : C \longrightarrow \mathbb{P}^1$ be a simple Hurwitz cover of genus $g$ and degree $d$ with labeled profile $(\mu_i, \dots, \mu_n)$ over $\infty$, unramified over $0 \in \mathbb{P}^1$, and simply ramified over $B = \{\xi^1, \dots, \xi^s\} \subset \mathbb{P}^1$, where $\xi = \exp(2\pi i/s)$ and $s = 2g - 2 + d + n$. We denote by $R = \{p_1, \dots, p_s\} \subset C$ the labeled simple ramification points of $f$, that is bijectively mapped to $B$ by $f : R \longrightarrow B$. We choose a labeling of $R$ so that $f(p_\alpha) = \xi^\alpha$ for every $\alpha = 1, \dots, s$.

On $\mathbb{P}^1$, plot $B$ and connect each element $\xi^\alpha \in B$ with 0 by a straight line segment. We also connect 0 and $\infty$ by a straight line $z = t\exp(\pi i/s)$, $0 \le t \le \infty$. Let $*$ denote the configuration of the $s$ line segments. The inverse image $f^{-1}(*)$ is a cell graph on $C$, for which $f^{-1}(0)$ forms the set of vertices. We remove all inverse images $f^{-1}(\overline{0\xi^\alpha})$ of the line segment $\overline{0\xi^\alpha}$ from this graph, except for the ones that end at one of the points $p_\alpha \in R$. Since $p_\alpha$ is a simple ramification point of $f$, the line segment ending at $p_\alpha$ extends to another vertex, i.e., another point in $f^{-1}(0)$. We denote by $\gamma^\vee$ the graph after this removal of line segments. We define the edges of the graph to be the connected line segments at $p_\alpha$ for some $\alpha$. We use $p_\alpha$ as the label of the edge. The graph $\gamma^\vee$ has $d$ vertices, $s$ edges, and $n$ faces.

An inverse image of the line $\overline{0\infty}$ is a ray starting at a vertex of the graph $\gamma^\vee$ and ending up with one of the points in $f^{-1}(\infty)$, which is the center of a face. We place a dot on this line near at each vertex. The edges of $\gamma^\vee$ incident to a vertex are cyclically ordered counter-clockwise, following the natural cyclic order of $B$. Let $p_\alpha$ be an edge incident to a vertex, and $p_\beta$ the next one at the same vertex according to the cyclic order. We denote by $d_{\alpha\beta}$ the number of dots in the span of two edges $p_\alpha$ and $p_\beta$, which is 0 if $\alpha < \beta$, and 1 if $\beta < \alpha$. Now we consider the dual graph $\gamma$ of $\gamma^\vee$. It has $n$ vertices, $d$ faces, and $s$ edges still labeled by $\{p_1, \dots, p_s\}$. At the angled corner between the two adjacent edges labeled by $p_\alpha$ and $p_\beta$ in this order according to the cyclic order, we place $d_{\alpha\beta}$ dots. The data $(\gamma, D)$ consisting of the cell graph $\gamma$ and the dot configuration $D$ is the Hurwitz graph corresponding to the simple Hurwitz cover $f : C \longrightarrow \mathbb{P}^1$ for $r = 1$.

It is obvious that what we obtain is an $r = 1$ Hurwitz graph, except for the condition (5) of the configuration $D$, which requires an explanation. The dual graph $\gamma^\vee$ for $r = 1$ is the *branching graph* of [29]. Since $|B| = s$ is the number of simple ramification points, which is also the number of edges of $\gamma^\vee$, the branching graph cannot have any loops. This is because two distinct powers of $\xi$ in the range of $1, \dots, s$ cannot be the same. This fact reflects in the condition that $\gamma$ has no edge that bounds the same face twice. This explains the condition (5) for $r = 1$.

**Remark 6.4.** If we consider the case $r = 1, g = 0$ and $n = 1$, then $s = d - 1$. Hence the graph $\gamma^\vee$ is a connected tree consisting of $d$ nodes (vertices) and $d - 1$ *labeled* edges. Except for $d = 1, 2$, every vertex is uniquely labeled by incident edges. The tree counting of Introduction is relevant to Hurwitz numbers in this way.

6.3. **Construction of $r$-Hurwitz graphs for $r > 1$.** This time we consider an orbifold Hurwitz cover $f : C \longrightarrow \mathbb{P}^1[r]$ of genus $g$ and degree $d = rm$ with labeled profile $(\mu_i, \dots, \mu_n)$ over $\infty$, $m$ isomorphic stacky points over $\left[0\big/\big(\mathbb{Z}/(r)\big)\right] \in \mathbb{P}^1[r]$, and simply ramified over $B = \{\xi^1, \dots, \xi^s\} \subset \mathbb{P}^1[r]$, where $s = 2g - 2 + m + n$. By $R = \{p_1, \dots, p_s\} \subset C$ we indicate the labeled simple ramification points of $f$, that is again bijectively mapped to $B$ by $f : R \longrightarrow B$. We choose the same labeling of $R$ so that $f(p_\alpha) = \xi^\alpha$ for every $\alpha = 1, \dots, s$.

On $\mathbb{P}^1[r]$, plot $B$ and connect each element $\xi^\alpha \in B$ with the stacky point at 0 by a straight line segment. We also connect 0 and $\infty$ by a straight line $z = t\exp(\pi i/s)$, $0 \le t \le \infty$, as before. Let $*$ denote the configuration of the $s$ line segments. The inverse image $f^{-1}(*)$ is a cell graph on $C$, for which $f^{-1}(0)$ forms the set of vertices. We remove all inverse images $f^{-1}(\overline{0\xi^\alpha})$ of the line segment $\overline{0\xi^\alpha}$ from this graph, except for the ones that end at one of the points $p_\alpha \in R$. We denote by $\gamma^\vee$ the graph after this removal of line segments. We define the edges of the graph to be the connected line segments at $p_\alpha$ for some $\alpha$. We use $p_\alpha$ as the label of the edge. The graph $\gamma^\vee$ has $m$ vertices, $s$ edges.

The inverse image of the line $\overline{0\infty}$ form a set of $r$ rays at each vertex of the graph $\gamma^\vee$, connecting $m$ vertices and $n$ centers $f^{-1}(\infty)$ of faces. We place a dot on each line near at each vertex. These dots are cyclically ordered according to the orientation of $C$, which we choose to be counter-clock wise. The edges of $\gamma^\vee$ incident to a vertex are also cyclically ordered in the same way. Let $p_\alpha$ be an edge incident to this vertex, and $p_\beta$ the next one according to the cyclic order. We denote by $d_{\alpha\beta}$ the number of dots in the span of two edges $p_\alpha$ and $p_\beta$. Let $\gamma$ denote the dual graph of $\gamma^\vee$. It now has $n$ vertices, $m$ faces, and $s$ edges still labeled by $\{p_1, \dots, p_s\}$. At the angled corner between the two adjacent edges labeled by $p_\alpha$ and $p_\beta$ in this order according to the cyclic order, we place $d_{\alpha\beta}$ dots, again cyclically ordered as on $\gamma^\vee$. The data $(\gamma, D)$ consisting of the cell graph $\gamma$ and the dot configuration $D$ is the $r$-Hurwitz graph corresponding to the orbifold Hurwitz cover $f : C \longrightarrow \mathbb{P}^1[r]$.

We note that $\gamma^\vee$ can have loops, unlike the case of $r = 1$. Let us place $\gamma^\vee$ locally on an oriented plane around a vertex. The plane is locally separated into $r$ sectors by the $r$ rays $f^{-1}(\overline{0\infty})$ at this vertex. There are $s$ half-edges coming out of the vertex at each of these $r$ sectors. A half-edge corresponding to $\xi^\alpha$ cannot be connected to another half-edge corresponding to $\xi^\beta$ in the same sector, by the same reason for the case of $r = 1$. But it can be connected to another half-edge of a different sector corresponding again to the same $\xi^\alpha$. In this case, within the loop there are some dots, representing the rays of $f^{-1}(\overline{0\infty})$ in between these half-edges. The total number of dots in the loop cannot be $r$, because then the half-edges being connected are in the same sector. Thus the condition (5) is satisfied.

6.4. **An example.** Theorem 6.7 below shows that

$$\mathcal{H}^2_{0,2}(3,1) = \frac{9}{2}.$$

This is the weighted count of the number of 2-Hurwitz graphs of type $(g, n, d) = (0, 2, 4)$ with an ordered partition $4 = 3 + 1$.

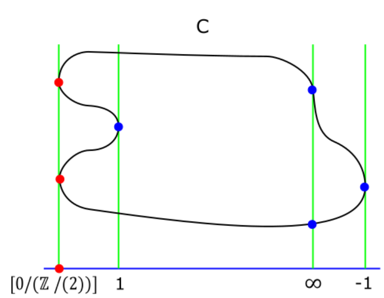


FIGURE 6.2. Hurwitz covers counted in $\mathcal{H}^2_{0,2}(3,1)$ have two orbifolds points, two simple ramification points, and one ramification point of degree 3.

In terms of formulas, the 2-Hurwitz cover corresponding to the graph on the left of Figure 6.3 is given by

$$f(x) = \frac{(x-1)^2(x+1)^2}{x}.$$

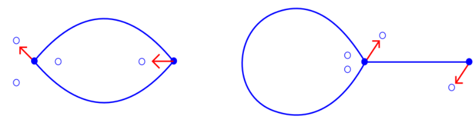

FIGURE 6.3. There are two 2-Hurwitz graphs. The number of graphs is $3/2$ for the graph on the left counting the automorphism, and 3 for the one on the right. The total is thus $9/2$.

To make the simple ramification points sit on $\pm 1$, we need to divide $f(x)$ by $f(i/\sqrt{3})$, where $x = \pm 1/\sqrt{3}$ are the simple ramification points. The 2-Hurwitz cover corresponding to the graph on the right of Figure 6.3 is given by

$$f(x) = \frac{(x-1)^2(x+1)^2}{x-a},$$

where $a$ is a real number satisfying $|a| > \sqrt{3}/2$. The real parameter $a$ changes the topological type of the 2-Hurwitz cover. For $-\frac{\sqrt{3}}{2} < a < \frac{\sqrt{3}}{2}$, the graph is the same as on the left, and for $|a| > \frac{\sqrt{3}}{2}$, the graph becomes the one on the right.

6.5. **The edge-contraction formulas.**

**Definition 6.5** (Edge-contraction operations)**.** The edge-contraction operations (ECOs) on an arrowed $r$-Hurwitz graph $(\gamma, \vec{D})$ are the following procedures. Choose an edge $E$ of the cell graph $\gamma$.

- **ECO 1**: We consider the case that $E$ is an edge connecting two distinct vertices Vertex $i$ and Vertex $j$. We can assume $i < j$, which induces a direction $i \xrightarrow{E} j$ on $E$. Let us denote by $F_+$ and $F_-$ the faces bounded by $E$, where $F_+$ is on the left side of $E$ with respect to the direction. We now contract $E$, with the following additional operations:
  (1) Remove the original arrows at Vertices $i$ and $j$.
  (2) Put the dots on $F_\pm$ clustered at Vertices $i$ and $j$ together, keeping the cyclic order of the dots on each of $F_\pm$.
  (3) Place a new arrow to the largest dot on the corner at Vertex $i$ of Face $F_+$ with respect to the cyclic order.
  (4) If there are no dots on this particular corner, then place an arrow to the first dot we encounter according to the counter-clock wise rotation from $E$ and centered at Vertex $i$.

The new arrow at the joined vertex allows us to recover the original graph from the new one.

- **ECO 2**: This time $E$ is a loop incident to Vertex $i$ twice. We contract $E$ and separate the vertex into two new ones, as in ECA 3 of Definition 4.4. The additional operations are:
  (1) The contraction of a loop does not change the number of faces. Separate the dots clustered at Vertex $i$ according to the original configuration.
  (2) Look at the new vertex to which the original arrow is placed. We keep the same name $i$ to this vertex. The other vertex is named $i'$.
  (3) Place a new arrow to the dot on the corner at the new Vertex $i$ that was the largest in the original corner with respect to the cyclic order.

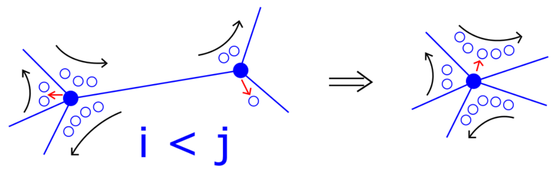


FIGURE 6.4. After contracting the edge, a new arrow is placed on the dot that is the largest (according to the cyclic order) around Vertex $i$ in the original graph, and on the face incident to $E$ which is on the left of $E$ with respect to the direction $i \to j$. The new arrow tells us where the break is made in the original graph. If there are no dots on this particular face, then we go around Vertex $i$ counter-clock wise and find the first dot in the original graph. We place an arrow to this dot in the new graph after contracting $E$. Here again the purpose is to identify which of the $\mu_i$ dots come from the original Vertex $i$

(4) If there are no dots on this particular corner, then place an arrow to the first dot we encounter according to the counter-clock wise rotation from $E$ and centered at Vertex $i$ on the side of the old arrow.
(5) We do the same operation for the new Vertex $i'$, and put a new arrow to a dot.
(6) Now remove the original arrow.

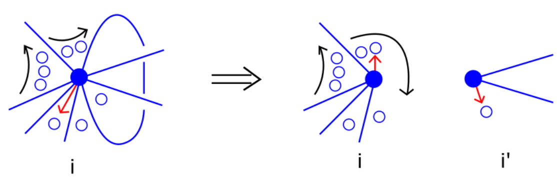


FIGURE 6.5. New arrows are placed so that the original graph can be recovered from the new one

Although cumbersome, it is easy to show that

**Lemma 6.6.** *The edge-contraction operations preserve the set of $r$-Hurwitz graphs.*

An application of the edge-contraction operations is the following counting recursion formula.

**Theorem 6.7** (Edge-Contraction Formula)**.** *The number of arrowed Hurwitz graphs satisfy the following edge-contraction formula.*

$$\begin{aligned}
&\left(2g-2+\frac{d}{r}+n\right)\mathcal{H}^r_{g,n}(\mu_1\dots,\mu_n)\\
&\quad=\sum_{i<j}\mu_i\mu_j\mathcal{H}^r_{g,n-1}(\mu_1,\dots,\mu_{i-1},\mu_i+\mu_j,\mu_{i+1},\dots,\widehat{\mu_j},\dots,\mu_n)\\
&\quad+\frac{1}{2}\sum_{i=1}^n\mu_i\sum_{\substack{\alpha+\beta=\mu_i\\ \alpha,\beta\geq 1}}\Bigg[\mathcal{H}^r_{g-1,n+1}(\alpha,\beta,\mu_1,\dots,\widehat{\mu_i},\dots,\mu_n)\\
&\quad+\sum_{\substack{g_1+g_2=g\\ I\sqcup J=\{1,\dots,\hat{i},\dots,n\}}}\mathcal{H}^r_{g_1,|I|+1}(\alpha,\mu_I)\mathcal{H}^r_{g_2,|J|+1}(\beta,\mu_J)\Bigg].
\end{aligned}\tag{6.4}$$

*Here,* $\widehat{\ }$ *indicates the omission of the index, and* $\mu_I=(\mu_i)_{i\in I}$ *for any subset* $I\subset\{1,2,\dots,n\}$.

**Remark 6.8.** The edge-contraction formula (ECF) is a recursion with respect to the number of edges

$$s=2g-2+\frac{\mu_1+\cdots+\mu_n}{r}+n.$$

Therefore, it calculates all values of $\mathcal{H}^r_{g,n}(\mu_1\dots,\mu_n)$ from the base case $\mathcal{H}^r_{0,1}(r)$. However, it does not determine the initial value itself, since $s=0$. We also note that the recursion is not for $\mathcal{H}^r_{g,n}$ as a function in $n$ integer variables.

*Proof.* The counting is done by applying the edge-contraction operations. The left-hand side of (6.4) shows the choice of an edge, say $E$, out of $s=2g-2+\frac{d}{r}+n$ edges. The first line of the right-hand side corresponds to the case that the chosen edge $E$ connects Vertex $i$ and Vertex $j$. We assume $i<j$, and apply ECO 1. The factor $\mu_i\mu_j$ indicates the removal of two arrows at these vertices (Figure 6.4).

When the edge $E$ we have chosen is a loop incident to Vertex $i$ twice, then we apply ECO 2. The factor $\mu_i$ is the removal of the original arrow (Figure 6.5). The second and third lines on the right-hand side correspond whether $E$ is a handle-cutting loop, or a separation loop. The factor $\frac{1}{2}$ is there because of the symmetry between $\alpha$ and $\beta$ of the partition of $\mu_i$. This complete the proof. □

**Theorem 6.9** (Graph enumeration and orbifold Hurwitz numbers)**.** *The graph enumeration and counting orbifold Hurwitz number are related by the following formula:*

$$\mathcal{H}^r_{g,n}(\mu_i,\dots,\mu_n)=\mu_1\mu_2\cdots\mu_n H^r_{g,n}(\mu_i,\dots,\mu_n).\tag{6.5}$$

*Proof.* The simplest orbifold Hurwitz number is $H^r_{0,1}(r)$, which counts double Hurwitz numbers with the same profile $(r)$ at both $0\in\mathbb{P}^1$ and $\infty\in\mathbb{P}^1$. There is only one such map $f:\mathbb{P}^1\longrightarrow\mathbb{P}^1$, which is given by $f(x)=x^r$. Since the map has automorphism $\mathbb{Z}/(r)$, we have $H^r_{0,1}(r)=1/r$. Thus (6.5) holds for the base case.

We notice that (6.4) is exactly the same as the cut-and-join equation of [4, Theorem 2.2], after modifying the orbifold Hurwitz numbers by multiplying $\mu_1\cdots\mu_n$. Since the initial value is the same, and the formulas are recursion based on $s=2g-2+\frac{d}{r}+n$, (6.5) holds by induction. This completes the proof. □

## 7. Construction of the mirror spectral curves for orbifold Hurwitz numbers

In the earlier work on simple and orbifold Hurwitz numbers in connection to the topological recursion [4, 5, 8, 14, 27], the spectral curves are determined by the infinite framing limit of the mirror curves to toric Calabi-Yau (orbi-)threefolds. The other ingredients of the topological recursion, the differential forms $W_{0,1}$ and $W_{0,2}$, are calculated by the Laplace transform of the $(g,n) = (0,1)$ and $(0,2)$ cases of the ELSV [13] and JPT [18] formulas. Certainly the logic is clear, but why these choices are the right ones is not well explained.

In this section, we show that the edge-contraction operations themselves determine all the mirror ingredients, i.e., the spectral curve, $W_{0,1}$, and $W_{0,2}$. The structure of the story is the following. The edge-contraction formula (6.4) is an equation among different values of $(g,n)$. When restricted to $(g,n) = (0,1)$, it produces an equation on $\mathcal{H}^r_{0,1}(d)$ as a function in one integer variable. The generating function of $\mathcal{H}^r_{g,n}(\mu_1,\dots,\mu_n)$ is reasonably complicated, but it can be expressed rather nicely in terms of the generating function of the $(0,1)$-values $\mathcal{H}^r_{0,1}(d)$, which is essentially the spectral curve of the theory. The edge-contraction formula (6.4) itself has the Laplace transform that can be calculated in the spectral curve coordinate. Since (6.4) contains $(g,n)$ on each side of the equation, to make it a genuine recursion formula for functions with respect to $2g-2+n$ in the stable range, we need to calculate the generating functions of $\mathcal{H}^r_{0,1}(d)$ and $\mathcal{H}^r_{0,2}(\mu_1,\mu_2)$, and make the rest of (6.4) free of unstable terms. The result is the topological recursion of [4, 14].

Let us now start with the restricted (6.4) on $(0,1)$ invariants:

$$\left(\frac{d}{r}-1\right)\mathcal{H}^r_{0,1}(d) = \frac{1}{2}d\sum_{\substack{\alpha+\beta=d\\ \alpha,\beta\geq 1}}\mathcal{H}^r_{0,1}(\alpha)\mathcal{H}^r_{0,1}(\beta). \tag{7.1}$$

At this stage, we introduce a generating function

$$y = y(x) = \sum_{d=1}^{\infty}\mathcal{H}^r_{0,1}(d)x^d. \tag{7.2}$$

In terms of this generating function, (7.1) is a differential equation

$$\left(x^{r+1}\circ\frac{d}{dx}\circ\frac{1}{x^r}\right)y = \frac{1}{2}rx\frac{d}{dx}y^2, \tag{7.3}$$

or simply

$$\frac{y'}{y} - ry' = \frac{r}{x}.$$

Its unique solution is

$$Cx^r = ye^{-ry}$$

with a constant of integration $C$. As we noted in the previous section, the recursion (6.4) does not determine the initial value $\mathcal{H}^r_{0,1}(d)$. For our graph enumeration problem, the values are

$$\mathcal{H}^r_{0,1}(d) = \begin{cases} 0 & 1\leq d<r;\\ 1 & d=r,\end{cases} \tag{7.4}$$

which determine $C=1$. Thus we find

$$x^r = ye^{-ry}, \tag{7.5}$$

which is the $r$-Lambert curve of [4]. This is indeed the spectral curve for the orbifold Hurwitz numbers.

**Remark 7.1.** We note that $r\mathcal{H}^r_{0,1}(rm)$ satisfies the same recursion equation (7.1) for $r = 1$, with a different initial value. Thus essentially orbifold Hurwitz numbers are determined by the usual simple Hurwitz numbers.

**Remark 7.2.** If we define $T_d = (d-1)!\mathcal{H}^{r=1}_{0,1}(d)$, then (7.1) for $r = 1$ is equivalent to (1.1). This is the reason we consider the tree recursion as the spectral curve for simple and orbifold Hurwitz numbers.

For the purpose of performing analysis on the spectral curve (7.5), let us introduce a global coordinate $z$ on the $r$-Lambert curve, which is an analytic curve of genus 0:

$$\begin{cases} x = x(z) := ze^{-z^r} \\ y = y(z) := z^r. \end{cases} \tag{7.6}$$

We denote by $\Sigma \subset \mathbb{C}^2$ this parametric curve. Let us introduce the generating functions of general $\mathcal{H}^r_{g,n}$, which are called *free energies*:

$$F_{g,n}(x_1, \dots, x_n) := \sum_{\mu_1,\dots,\mu_n \geq 1} \frac{1}{\mu_1 \cdots \mu_n} \mathcal{H}^r_{g,n}(\mu_1, \dots, \mu_n) \prod_{i=1}^n x_i^{\mu_i}. \tag{7.7}$$

We also define the exterior derivative

$$W_{g,n}(x_1, \dots, x_n) := d_1 \cdots d_n F_{g,n}(x_1, \dots, x_n), \tag{7.8}$$

which is a symmetric $n$-linear differential form. By definition, we have

$$y = y(x) = x \frac{d}{dx} F_{0,1}(x). \tag{7.9}$$

The topological recursion requires the spectral curve, $W_{0,1}$, and $W_{0,2}$. From (7.8) and (7.9), we have

$$W_{0,1}(x) = y\frac{dx}{x} = y d\log(x). \tag{7.10}$$

**Remark 7.3.** For many examples of topological recursion such as ones considered in [12], we often define $W_{0,1} = ydx$, which is a holomorphic 1-form on the spectral curve. For Hurwitz theory, due to (7.9), it is more natural to use (7.10).

As a differential equation, we can solve (7.9) in a closed formula on the spectral curve $\Sigma$ of (7.6). Indeed, the role of the spectral curve is that the free energies, i.e., $F_{g,n}$'s, are actually analytic functions defined on $\Sigma^n$. Although we define $F_{g,n}$'s as a formal power series in $(x_1, \dots, x_n)$ as generating functions, they are analytic, and the domain of analyticity, or the classical sense of *Riemann surface*, is the spectral curve $\Sigma$. The coordinate change (7.6) gives us

$$x\frac{d}{dx} = \frac{z}{1 - rz^r}\frac{d}{dz}, \tag{7.11}$$

hence (7.9) is equivalent to

$$z^{r-1}(1 - rz^r) = \frac{d}{dz} F_{0,1}\big(x(z)\big).$$

Since $z = 0 \Longrightarrow x = 0 \Longrightarrow F_{0,1}(x) = 0$, we find

$$F_{0,1}\big(x(z)\big) = \frac{1}{r}z^r - \frac{1}{2}z^{2r}. \tag{7.12}$$

The calculation of $F_{0,2}$ is done similarly, by restricting (6.4) to the $(g,n)=(0,1)$ and $(0,2)$ terms. Assuming that $\mu_1+\mu_n=mr$, we have

$$\begin{aligned}(7.13)\quad &\left(\frac{d}{r}-1\right)\mathcal{H}^r_{0,2}(\mu_1,\mu_2)\\ &=\mu_1\mu_2\mathcal{H}^r_{0,1}(\mu_1+\mu_2)+\mu_1\sum_{\substack{\alpha+\beta=\mu_1\\ \alpha,\beta>0}}\mathcal{H}^r_{0,1}(\alpha)\mathcal{H}^r_{0,2}(\beta,\mu_2)+\mu_2\sum_{\substack{\alpha+\beta=\mu_2\\ \alpha,\beta>0}}\mathcal{H}^r_{0,1}(\alpha)\mathcal{H}^r_{0,2}(\mu_1,\beta).\end{aligned}$$

As a special case of [4, Lemma 4.1], this equation translates into a differential equation for $F_{0,2}$:

$$\begin{aligned}(7.14)\quad &\frac{1}{r}\left(x_1\frac{\partial}{\partial x_1}+x_2\frac{\partial}{\partial x_2}\right)F_{0,2}(x_1,x_2)\\ &=\frac{1}{x_1-x_2}\left(x_1^2\frac{\partial}{\partial x_1}F_{0,1}(x_1)-x_2^2\frac{\partial}{\partial x_2}F_{0,1}(x_2)\right)-\left(x_1\frac{\partial}{\partial x_1}F_{0,1}(x_1)+x_2\frac{\partial}{\partial x_2}F_{0,1}(x_2)\right)\\ &+\left(x_1\frac{\partial}{\partial x_1}F_{0,1}(x_1)\right)\left(x_1\frac{\partial}{\partial x_1}F_{0,2}(x_1,x_2)\right)+\left(x_2\frac{\partial}{\partial x_2}F_{0,1}(x_2)\right)\left(x_2\frac{\partial}{\partial x_2}F_{0,2}(x_1,x_2)\right).\end{aligned}$$

Denoting by $x_i=x(z_i)$ and using (7.11), (7.14) becomes simply

$$(7.15)\qquad \frac{1}{r}\left(z_1\frac{\partial}{\partial z_1}+z_2\frac{\partial}{\partial z_2}\right)F_{0,2}\big(x(z_1),x(z_2)\big)=\frac{x_1z_1^r-x_2z_2^r}{x_1-x_2}-(z_1^r+z_2^r)$$

on the spectral curve $\Sigma$. This is a linear partial differential equation of the first order with analytic coefficients in the neighborhood of $(0,0)\in\mathbb{C}^2$, hence by the Cauchy-Kovalevskaya theorem, it has the unique analytic solution around the origin of $\mathbb{C}^2$ for any Cauchy problem. Since the only analytic solution to the homogeneous equation

$$\left(z_1\frac{\partial}{\partial z_1}+z_2\frac{\partial}{\partial z_2}\right)f(z_1,z_2)=0$$

is a constant, the initial condition $F_{0,2}(0,x_2)=F_{0,2}(x_1,0)=0$ determines the unique solution of (7.15).

**Proposition 7.4.** *We have a closed formula for $F_{0,2}$ in the $z$-coordinates:*

$$(7.16)\qquad F_{0,2}\big(x(z_1),x(z_2)\big)=\log\frac{z_1-z_2}{x(z_1)-x(z_2)}-(z_1^r+z_2^r).$$

*Proof.* We first note that $\log\frac{z_1-z_2}{x(z_1)-x(z_2)}$ is holomorphic around $(0,0)\in\mathbb{C}^2$. (7.16) being a solution to (7.15) is a straightforward calculation that can be verified as follows:

$$\begin{aligned}&\left(z_1\frac{\partial}{\partial z_1}+z_2\frac{\partial}{\partial z_2}\right)\log\frac{z_1-z_2}{x(z_1)-x(z_2)}\\ &=\frac{z_1-z_2}{z_1-z_2}-\frac{z_1e^{-z_1^r}(1-rz_1^r)-z_2e^{-z_2^r}(1-rz_2^r)}{x_1-x_2}\\ &=1-\frac{x_1-x_2}{x_1-x_2}+r\frac{x_1z_1^r-x_2z_2^r}{x_1-x_2}=r\frac{x_1z_1^r-x_2z_2^r}{x_1-x_2}.\end{aligned}$$

Since $F_{0,2}\big(x(0),x(z_2)\big)=\log e^{z_2^r}-z_2^r=0$, (7.16) is the desired unique solution. $\square$

In [4], the functions (7.12) and (7.16) are derived by directly computing the Laplace transform of the JPT formulas [18]

$$
\begin{aligned}
H^r_{0,1}(d) &= \frac{d^{\lfloor \frac{d}{r} \rfloor -2}}{\lfloor \frac{d}{r} \rfloor !},\\
H^r_{0,2}(\mu_1,\mu_2) &= \begin{cases} r^{\langle \frac{\mu_1}{r}\rangle + \langle \frac{\mu_1}{r}\rangle} \frac{1}{\mu_1+\mu_2} \frac{\mu_1^{\lfloor \frac{\mu_1}{r}\rfloor} \mu_2^{\lfloor \frac{\mu_2}{r}\rfloor}}{\lfloor \frac{\mu_1}{r}\rfloor ! \lfloor \frac{\mu_2}{r}\rfloor !} & \mu_1+\mu_2 \equiv 0 \mod r\\ 0 & \text{otherwise.}\end{cases}
\end{aligned}
\tag{7.17}
$$

Here, $q = \lfloor q \rfloor + \langle q \rangle$ gives the decomposition of a rational number $q \in \mathbb{Q}$ into its floor and the fractional part. We have thus recovered (7.17) from the edge-contraction formula alone, which are the $(0,1)$ and $(0,2)$ cases of the ELSV formula for the orbifold Hurwitz numbers.

**Acknowledgement.** The authors are grateful to the American Institute of Mathematics in California, the Banff International Research Station, the Institute for Mathematical Sciences at the National University of Singapore, Kobe University, Leibniz Universität Hannover, the Lorentz Center for Mathematical Sciences, Leiden, and Max-Planck-Institut für Mathematik in Bonn, for their hospitality and financial support during the authors' stay for collaboration. They thank Ruian Chen, Maxim Kontsevich and Shintaro Yanagida for valuable discussions. They also thank the referee for useful comments in improving the manuscript. O.D. thanks the Perimeter Institute for Theoretical Physics, and M.M. thanks the Hong Kong University of Science and Technology and the Simons Center for Geometry and Physics, for financial support and hospitality. The research of O.D. has been supported by GRK 1463 *Analysis, Geometry, and String Theory* at Leibniz Universität Hannover. The research of M.M. has been supported by NSF grants DMS-1104734, DMS-1309298, and NSF-RNMS: Geometric Structures And Representation Varieties (GEAR Network, DMS-1107452, 1107263, 1107367).

## References


[1] L. Abrams, *Two-dimensional topological quantum field theories and Frobenius algebras*, Journal of Knot Theory and Ramifications **5**, 335–352 (2000).

[2] M.F. Atiyah, *Topological quantum field theory*, [arXiv:hep-th/0312085], Publications Mathématiques de l'I.H.É.S., **68**, 175–186 (1988).

[3] G. V. Belyi, *On galois extensions of a maximal cyclotomic fields*, Math. U.S.S.R. Izvestija **14**, 247–256 (1980).

[4] V. Bouchard, D. Hernández Serrano, X. Liu, and M. Mulase, *Mirror symmetry for orbifold Hurwitz numbers*, arXiv:1301.4871 [math.AG] (2013).

[5] V. Bouchard and M. Mariño, *Hurwitz numbers, matrix models and enumerative geometry*, Proc. Symposia Pure Math. **78**, 263–283 (2008).

[6] R. Chen, *Topological quantum field theory from the viewpoint of cellular graphs*, Senior Thesis, University of California, Davis (2015).

[7] R. Dijkgraaf, E. Verlinde, and H. Verlinde, *Loop equations and Virasoro constraints in non-perturbative two-dimensional quantum gravity*, Nucl. Phys. **B348**, 435–456 (1991).

[8] N. Do, O. Leigh, and P. Norbury, *Orbifold Hurwitz numbers and Eynard-Orantin invariants*, arXiv:1212.6850 (2012).

[9] O. Dumitrescu and M. Mulase, *Quantum curves for Hitchin fibrations and the Eynard-Orantin theory*, Lett. Math. Phys. **104**, 635–671 (2014).

[10] O. Dumitrescu and M. Mulase, *Quantization of spectral curves for meromorphic Higgs bundles through topological recursion*, arXiv:1411.1023 (2014).

[11] O. Dumitrescu and M. Mulase, *Lectures on the topological recursion for Higgs bundles and quantum curves*, to appear in the lecture notes series of the National University of Singapore.

[12] O. Dumitrescu, M. Mulase, A. Sorkin and B. Safnuk, *The spectral curve of the Eynard-Orantin recursion via the Laplace transform*, in "Algebraic and Geometric Aspects of Integrable Systems and Random Matrices," Dzhamay, Maruno and Pierce, Eds. Contemporary Mathematics **593**, 263–315 (2013).

[13] T. Ekedahl, S. Lando, M. Shapiro, A. Vainshtein, *Hurwitz numbers and intersections on moduli spaces of curves*, Invent. Math. **146**, 297–327 (2001) [arXiv:math/0004096].

[14] B. Eynard, M. Mulase and B. Safnuk, *The Laplace transform of the cut-and-join equation and the Bouchard-Mariño conjecture on Hurwitz numbers*, Publications of the Research Institute for Mathematical Sciences **47**, 629–670 (2011).

[15] B. Eynard and N. Orantin, *Invariants of algebraic curves and topological expansion*, Communications in Number Theory and Physics **1**, 347–452 (2007).

[16] A. Grothendieck, *Esquisse d'un programme*, (1984).

[17] J. L. Harer, *The cohomology of the moduli space of curves*, in Theory of Moduli, Montecatini Terme, 1985 (Edoardo Sernesi, ed.), Springer-Verlag, 1988, pp. 138–221.

[18] P. Johnson, R. Pandharipande, and H.H. Tseng, *Abelian Hurwitz-Hodge integrals*, Michigan Math. J. **60**, 171–198 (2011) [arXiv:0803.0499].

[19] J. Kock, *Frobenius algebras and 2D topological quantum field theories*, Cambridge University Press (2003).

[20] M. Kontsevich, *Intersection theory on the moduli space of curves and the matrix Airy function*, Communications in Mathematical Physics **147**, 1–23 (1992).

[21] M. Kontsevich and Yuri Manin, *Gromov-Witten classes, quantum cohomology, and enumerative geometry*, Communications in Mathematical Physics **164**, 525–562 (1994),

[22] M. Mirzakhani, *Simple geodesics and Weil-Petersson volumes of moduli spaces of bordered Riemann surfaces*, Invent. Math. **167**, 179–222 (2007).

[23] M. Mirzakhani, *Weil-Petersson volumes and intersection theory on the moduli space of curves*, J. Amer. Math. Soc. **20**, 1–23 (2007).

[24] M. Mulase and M. Penkava, *Ribbon graphs, quadratic differentials on Riemann surfaces, and algebraic curves defined over* $\overline{\mathbb{Q}}$, The Asian Journal of Mathematics **2** (4), 875–920 (1998).

[25] M. Mulase and M. Penkava, *Topological recursion for the Poincaré polynomial of the combinatorial moduli space of curves*, Advances in Mathematics **230**, 1322–1339 (2012).

[26] M. Mulase and P. Sułkowski, *Spectral curves and the Schrödinger equations for the Eynard-Orantin recursion*, arXiv:1210.3006 (2012).

[27] M. Mulase and N. Zhang, *Polynomial recursion formula for linear Hodge integrals*, Communications in Number Theory and Physics **4**, 267–294 (2010).

[28] D. Mumford, *Towards an enumerative geometry of the moduli space of curves* (1983), in "Selected Papers of David Mumford," 235–292 (2004).

[29] A. Okounkov and R. Pandharipande, *Gromov-Witten theory, Hurwitz numbers, and matrix models, I*, Proc. Symposia Pure Math. **80**, 325–414 (2009).

[30] G. Segal, *Geometric aspect of quantum field theory*, Proceedings of the International Congress of Mathematicians, Kyoto, Japan 1990, 1387–1396 (1991).

[31] D. D. Sleator, R. E. Tarjan, and W. P. Thurston, *Rotation distance, triangulations, and hyperbolic geometry*, Journal of the American Mathematical Society **1**, 647–681 (1988).

[32] K. Strebel, *Quadratic differentials*, Springer-Verlag, 1984.

[33] C. Teleman, *The structure of 2D semi-simple field theories*, Inventiones Mathematicae **188**, 525–588 (2012).

[34] G. 't Hooft, *A planer diagram theory for strong interactions*, Nuclear Physics **B 72**, 461–473 (1974).

[35] T.R.S. Walsh and A.B. Lehman, *Counting rooted maps by genus. I*, Journal of Combinatorial Theory **B-13**, 192–218 (1972).

[36] E. Witten, *Two dimensional gravity and intersection theory on moduli space*, Surveys in Differential Geometry **1**, 243–310 (1991).



O. Dumitrescu: Max-Planck-Institut für Mathematik, Bonn, Germany

Current Address: Department of Mathematics, Central Michigan University, Mount Pleasant, MI 48859

*E-mail address*: dumit1om@cmich.edu

Simion Stoilow Institute of Mathematics, Romanian Academy, 21 Calea Grivitei Street, 010702 Bucharest, Romania

M. Mulase: Department of Mathematics, University of California, Davis, CA 95616–8633

*E-mail address*: mulase@math.ucdavis.edu

Kavli Institute for Physics and Mathematics of the Universe, The University of Tokyo, Kashiwa, Japan